Instead, metalloporphyrin photochemistry arises from higher excited states that involve charge-transfer transitions, either from the axial ligand to the metal or from the porphyrin itself to the metal. The formation of metal–oxo species from photolysis of various metalloporphyrin oxoanion complexes in solutions derives from secondary, thermal reactions.

Spin Frustration: A Hexanuclear Ferric Complex with a $S = 5$ Ground State

James K. McCusker, Cheryl A. Christmas, Paula M. Hagen, Raj K. Chadha, Daniel F. Harvey,* and David N. Hendrickson*

Contribution from the Department of Chemistry, 0506, University of California, San Diego, La Jolla, California 92093-0506. Received July 16, 1990

Abstract: The preparation and characterization of a hexanuclear Fe^{III} complex possessing an unusual $S = 5$ ground state are described. Reaction of 1,1-bis(N-methylimidazol-2-yl)-1-hydroxyethane (**1**) with $[Fe_3O(OAc)_6L_3]X$ (**2**), where L = pyridine or H_2O and X = ClO_4^- or NO_3^-, in CH_3CN followed by recrystallization in CH_2Cl_2 affords crystals of $[Fe_6O_2(OH)_2(O-Ac)_{10}(C_{10}H_{13}N_4O)_2]\cdot xCH_2Cl_2$ (**3**·xCH_2Cl_2). Complex **3**·$8CH_2Cl_2$ crystallizes in the triclinic space group $P\bar{1}$ with $a = 12.167$ (2) Å, $b = 12.921$ (4) Å, $c = 15.394$ (4) Å, $\alpha = 114.41$ (2)°, $\beta = 97.641$ (15)°, $\gamma = 102.17$ (2)°, $V = 2087.4$ (8) Å³, and $Z = 1$ at −100 °C. The structure was refined with 4179 observed reflections ($F > 6.0\sigma$) to give $R = 0.0465$ and $R_w = 0.0591$. The molecule resides at a center of inversion, making only three of the iron ions unique. Two of the iron ions have O_6 coordination spheres, while the third has an O_5N environment due to binding by one of the imidazole nitrogen atoms; the second imidazole ring of complex **1** remains uncoordinated. Complex **3** consists of two μ_3-oxo Fe^{III}_3 triangular complexes bridged together at two vertices by two μ_2-OH and four μ_2-O_2CCH_3 ions. ^{57}Fe Mössbauer data can be fit to two quadrupole-split doublets in a 2:1 area ratio with $\delta = 0.383$ (3) and 0.406 (6) mm/s and $\Delta E_Q = 0.729$ (5) and 1.056 (11) mm/s, respectively, at 300 K. The parameters are consistent with high-spin Fe^{III}. Magnetic susceptibility data at 10.00 kG in the temperature range 6–350 K reveal an increase in effective moment with decreasing temperature from 9.21 μ_B at 346.1 K to a maximum of 10.90 μ_B at 20.00 K. Variable-field magnetization data measured to 1.57 K at 40.00 kG saturate at a reduced magnetization $M/N\mu_B$ of 9.2. Fitting of the magnetization data by full-matrix diagonalization and including axial zero-field interactions establish the ground state as having $S = 5$ with $g = 1.94$ and $D = 0.22$ cm⁻¹. The origin of this ground state is described in terms of spin frustration within the hexanuclear core, and the results are compared to those found for a similar hexanuclear complex for which a $S = 0$ ground state was found.

Introduction

Polynuclear oxo- or hydroxo-bridged transition-metal centers have been found in a variety of iron[1] and manganese[2] metalloproteins. Hemerythrin,[3] methane monooxygenase,[4] and ribonucleotide reductase[5] have diiron active sites with μ-oxo and μ-carboxylato bridges. In the course of making model complexes for these oxo–diiron protein sites, several interesting polynuclear ferric complexes with Fe_4, Fe_6, Fe_8, Fe_{10}, and Fe_{11} compositions

have been reported.[6] The largest nuclearity discrete oxo–hydroxo ferric complex is heteronuclear: $[Fe_{16}MO_{10}(OH)_{10}(O_2CPh)_{20}]$ (M = Mn^{II}, Co^{II}).[7] The pursuit of model complexes for the active sites of catalases and the water oxidation center of photosystem II has also yielded polynuclear manganese complexes with compositions of $Mn^{II}_2Mn^{III}_2$, $Mn^{II}Mn^{III}_3$, Mn^{III}_4, $Mn^{II}_4Mn^{III}_2$, Mn^{III}_8, $Mn^{II}Mn^{III}_8$, $Mn^{III}_4Mn^{IV}_6$, Mn^{II}_{12}, and $Mn^{III}_8Mn^{IV}_4$.[8] The most

(1) (a) Lippard, S. J. *Angew. Chem., Int. Ed. Engl.* **1988**, *27*, 344. (b) Lippard, S. J. *Chem. Br.* **1986**, *22*, 222. (c) Que, L.; Scarrow, R. C. In *Metal Clusters in Proteins*; Que, L., Ed.; ACS Symposium Series 372; American Chemical Society: Washington, DC, 1988; Chapter 8.

(2) (a) Christou, G. *Acc. Chem. Res.* **1989**, *22*, 328. (b) Dismukes, G. C. *Chem. Scr.* **1988**, *28*, 99. (c) Babcock, G. T. In *New Comprehensive Biochemistry: Photosynthesis*; Amesz, J., Ed.; Elsevier: Amsterdam, 1987; pp 125–158. (d) Brudvig, G. W.; Crabtree, R. H. *Prog. Inorg. Chem.* **1989**, *37*, 99. (e) Wieghardt, K. *Angew. Chem., Int. Ed. Engl.* **1989**, *28*, 1153.

(3) Wilkins, P. C.; Wilkins, R. G. *Coord. Chem. Rev.* **1987**, *79*, 195 and references therein.

(4) (a) Dalton, H. *Adv. Appl. Microbiol.* **1980**, *26*, 71. (b) Fox, B. G.; Surerus, K. K.; Münck, E.; Lipscomb, J. D. *J. Biol. Chem.* **1988**, *263*, 10553. (c) Ericson, A.; Hedman, B.; Hodgson, K. O.; Green, J.; Dalton, H.; Bentsen, J. G.; Beer, R. H.; Lippard, S. J. *J. Am. Chem. Soc.* **1988**, *110*, 2330.

(5) (a) Sjöberg, B.-M.; Gräslund, A. *Adv. Inorg. Biochem.* **1983**, *5*, 87. (b) Lammers, M.; Follmann, H. *Struct. Bonding (Berlin)* **1983**, *54*, 27.

(6) For examples of Fe_4 complexes see: (a) Murch, B. P.; Bradley, F. C.; Boyle, P. D.; Papaefthymiou, V.; Que, L., Jr. *J. Am. Chem. Soc.* **1987**, *109*, 7993. (b) Gorun, S. M.; Lippard, S. J. *Inorg. Chem.* **1988**, *27*, 149. (c) Drüeke, S.; Wieghardt, K.; Nuber, B.; Weiss, J.; Bominaar, E. L.; Sawaryn, A.; Winkler, H.; Trautwein, A. X. *Inorg. Chem.* **1989**, *28*, 4477. For examples of Fe_6 complexes see: (d) Batsanov, A. S.; Struchkov, Yu. T.; Timko, G. A. *Koord. Khim.* **1988**, *14*, 266. (e) Gérbéléu, N. V.; Batsanov, A. S.; Timko, G. A.; Struchkov, Yu. T.; Indrichan, K. M.; Popovich, G. A. *Dokl. Akad. Nauk SSSR* **1987**, *293*, 364. (f) Micklitz, W.; Lippard, S. J. *Inorg. Chem.* **1988**, *27*, 3067. (g) Micklitz, W.; Bott, S. G.; Bentsen, J. G.; Lippard, S. J. *J. Am. Chem. Soc.* **1989**, *111*, 372. (h) Hegetschweiler, K.; Schmalle, H.; Streit, H. M.; Schneider, W. *Inorg. Chem.* **1990**, *29*, 3625. For an example of an Fe_8 complex see: (i) Wieghardt, K.; Pohl, K.; Jibril, I.; Huttner, G. *Angew. Chem., Int. Ed. Engl.* **1984**, *23*, 77. For an example of a Fe_{10} complex see: (j) Taft, K. L.; Lippard, S. J. *J. Am. Chem. Soc.* **1990**, *112*, 9629. For examples of Fe_{11} complexes see: (k) Gorun, S. M.; Lippard, S. J. *Nature* **1986**, *319*, 666. (l) Gorun, S. M.; Papaefthymiou, G. C.; Frankel, R. B.; Lippard, S. J. *J. Am. Chem. Soc.* **1987**, *109*, 3337.

(7) Micklitz, W.; Lippard, S. J. *J. Am. Chem. Soc.* **1989**, *111*, 6856.

remarkable polynuclear ferric complex is found in the protein ferritin, which serves the role of iron storage, detoxification, and recycling.[9] The outer part of each ferritin molecule consists of 24 polypeptide units, existing as an apoprotein. The protein can store up to 4500 ferric ions inside a single molecule. Polymeric ferric complexes with molecular weights of $\sim 150\,000$, the "Saltman–Spiro balls", have been prepared[10] to model the ferric core of ferritin.

There are several intriguing features associated with oxo–hydroxo polynuclear manganese and iron complexes. First, these complexes can have unusual electronic structures. Even though the nature (antiferromagnetic or ferromagnetic) and magnitude of magnetic exchange interactions between two metal ions are reasonably well-understood in terms of the energetics and overlap of "magnetic orbitals",[11] there could be unusual magnetic exchange effects in these polynuclear complexes. There is already substantial evidence that the pairwise exchange interactions in these types of complexes cannot be totally explained by the Heisenberg–Dirac–Van Vleck (HDVV) Hamiltonian, $\hat{H} = -2J_{ij}\hat{S}_i\cdot\hat{S}_j$. Biquadratic and antisymmetric exchange[12] as well as double-exchange interactions[13] have been invoked to help describe the magnetic properties of certain complexes. Furthermore, as larger and larger complexes are prepared, it will be interesting to see whether unusual relaxation effects are observed for some of these molecules. The ferric core of ferritin, for example, exhibits the phenomenon of superparamagnetism.[9] Depending on the magnitude of the pairwise exchange interactions and the size of a given domain (i.e., region in a crystal where all the magnetic moments are aligned), the net magnetization of an assembly of metal ions (a molecule) may change direction at different rates in the solid.

A second general reason to study polynuclear metal complexes is that they may be building blocks for molecular-based magnetic materials.[14] At least three different approaches have been taken to prepare transition-metal complexes that behave as molecular ferromagnets. Miller and co-workers[15] have prepared organometallic ferromagnets that consist of metallocene cations and organic anions, each having one unpaired electron, assembled in alternating stacks. Kahn and co-workers[16] have prepared ferri-

magnetic chains comprising Cu^{II}–bridge–Mn^{II} units. The third approach was taken by Gatteschi et al.,[17] who prepared ferrimagnetic chains made of metal complexes with paramagnetic nitroxide ligands.

In general, molecules that have large numbers of unpaired electrons should serve as good starting points for constructing magnetic molecular materials. Iwamura et al.[18] and Itoh et al.[19] have prepared interesting organic molecules with conjugated π systems that have several unpaired electrons. Dougherty and co-workers[20] are preparing high-spin organic structures that have more localized bonding than found in the above conjugated π systems. A hydrocarbon consisting of five carbene linkages has the highest spin multiplicity for an organic molecule yet described, with $S = 5$.[18] Until recently, the $Mn^{II}_6(nitroxide)_6$ complex with $S = 12$ reported by Caneschi et al.[21] held the record for the largest spin ground state in a discrete molecular complex. This was replaced by $[Mn^{III}_8Mn^{IV}_4O_{12}(O_2CPh)_{16}(H_2O)_4]$, which has been shown[8f] to have a $S = 14$ ground state.

The topology of some of the polynuclear transition-metal complexes may be responsible for their high-spin ground states. For example, spin frustration can develop for a triangular arrangement of metal ions (vide infra). Even though the pairwise exchange interactions in these and other complexes are found to be antiferromagnetic or at best weakly ferromagnetic, spin frustration in a polynuclear complex can result in ground states having a relatively large number of unpaired electrons.[22] Spin frustration is a well-known magnetic exchange phenomenon for extended lattices. It has been recently reported[23] to be present in superconducting $YBa_2Cu_3O_{6+x}$ when x is in the range 0–0.3. It has also been noted that one of the two different Fe^{II} ions in the mixed-valence mineral ilvaite experiences spin frustration.[24] This Fe^{II} site occurs at the apex of a square pyramid, a site which can be viewed as being a corner ion common to two triangles.

In this paper we describe the preparation and characterization of a hexanuclear ferric complex, where each Fe^{III} ion is high-spin. It is shown that this Fe^{III}_6 complex exhibits unusual magnetochemistry. It is the first polynuclear complex containing only ferric ions that possesses an intermediate-spin ($S = 5$) ground state. Spin frustration is the likely origin of this novel $S = 5$ ground state.

Experimental Section

Compound Syntheses. All operations were carried out under aerobic conditions at ambient temperature unless otherwise indicated. N-Methylimidazole and ethyl acetate were distilled from CaH_2 before use. THF was freshly distilled from potassium/benzophenone ketyl. All other solvents and reagents were used as received unless otherwise indicated. Elemental analyses were performed by Galbraith Laboratories, by Oneida Research Services, or at the analytical facility of the UCSD Scripps Institute of Oceanography. *Warning: Though we have encountered no difficulties, appropriate care should be taken during the handling of the potentially explosive perchlorate salts.*

1,1-Bis(N-methylimidazol-2-yl)-1-hydroxyethane (1). To a solution of N-methylimidazole (6.30 mL, 79 mmol) in THF (400 mL) under N_2 at -78 °C was added n-BuLi (45 mL, 72 mmol, 1.6 M in hexane) dropwise via an addition funnel. After 30 min, EtOAc (2.37 mL, 24 mmol) was added and the solution was slowly warmed to room temperature and stirred for 10 h. After concentration in vacuo, the residue was dissolved in H_2O and extracted with $CHCl_3$. Recrystallization from 5:1 (v/v) $CHCl_3$/hexane at -22 °C gave white crystalline needles of **1** (2.98

(8) For examples of Mn₄ complexes see: (a) Vincent, J. B.; Christmas, C.; Chang, H.-R.; Li, Q.; Boyd, P. D. W.; Huffman, J. C.; Hendrickson, D. N.; Christou, G. *J. Am. Chem. Soc.* **1989**, *111*, 2086. For an example of a Mn₆ complex see: (b) Schake, A. R.; Vincent, J. B.; Li, Q.; Boyd, P. D. W.; Fotling, K.; Huffman, J. C.; Hendrickson, D. N.; Christou, G. *Inorg. Chem.* **1989**, *28*, 1915. For an example of a Mn₈ complex see: (c) Libby, E.; Folting, K.; Huffman, J. C.; Christou, G. *J. Am. Chem. Soc.* **1990**, *112*, 5354. For an example of a Mn₉ complex see: (d) Christmas, C.; Vincent, J. B.; Chang, H.-R.; Huffman, J. C.; Christou, G.; Hendrickson, D. N. *J. Am. Chem. Soc.* **1988**, *110*, 823. For an example of a Mn₁₀ complex see: (e) Hagen, K. S.; Armstrong, W. H.; Olmstead, M. M. *J. Am. Chem. Soc.* **1989**, *111*, 774. For examples of Mn₁₂ complexes see: (f) Boyd, P. D. W.; Li, Q.; Vincent, J. B.; Folting, K.; Chang, H.-R.; Streib, W. E.; Huffman, J. C.; Christou, G.; Hendrickson, D. N. *J. Am. Chem. Soc.* **1988**, *110*, 8537. (g) Lis, T. *Acta Crystallogr., Sect. B* **1980**, *B36*, 2042. (h) Luneau, D.; Savariault, J.-M.; Tuchagues, J.-P. *Inorg. Chem.* **1988**, *27*, 3912.

(9) Theil, E. C. *Annu. Rev. Biochem.* **1987**, *56*, 289 and references therein.

(10) Brady, G. W.; Kurkjian, C. R.; Lyden, E. F. X.; Robin, M. B.; Saltman, P.; Spiro, T.; Terzis, A. *Biochemistry* **1968**, *7*, 2185.

(11) *Magneto-Structural Correlation in Exchange-Coupled Systems*; Willett, R. D., Gatteschi, D., Kahn, O., Eds.; NATO ASI Series C, 140; D. Reidel Publishing Co.: Dordrecht, Holland, 1985.

(12) Tsukerblat, B. S.; Belinskii, M. I.; Fainzil'berg, V. E. *Sov. Sci. Rev., Sect. B* **1987**, *9*, 337.

(13) (a) Papaefthymiou, V.; Girerd, J.-J.; Moura, I.; Moura, J. J. G.; Münck, E. *J. Am. Chem. Soc.* **1987**, *109*, 4703. (b) Noodleman, L.; Case, D. A.; Sontum, S. F. *J. Chem. Phys.* **1989**, *86*, 743. (c) Drüeke, S.; Chaudhuri, P.; Pohl, K.; Wieghardt, K.; Ding, X.-Q.; Bill, E.; Sawaryn, A.; Trautwein, A. X.; Winkler, H.; Gurman, S. J. *J. Chem. Soc., Chem. Commun.* **1989**, 59. (d) Ding, X.-Q.; Bominaar, E. L.; Bill, E.; Winkler, H.; Trautwein, A. X.; Drüeke, S.; Chaudhuri, P.; Wieghardt, K. *J. Chem. Phys.* **1990**, *92*, 176.

(14) *Magnetic Molecular Materials*; Gatteschi, D., Ed.; Kluwer Academic Publishers, in press.

(15) (a) Miller, J. S.; Epstein, A. J.; Reiff, W. M. *Chem. Rev.* **1988**, *88*, 102 and references therein. (b) Miller, J. S.; Epstein, A. J.; Reiff, W. M. *Acc. Chem. Res.* **1988**, *21*, 114 and references therein.

(16) (a) Kahn, O. *Struct. Bonding (Berlin)* **1987**, *68*, 89 and references therein. (b) Kahn, O.; Pei, Y.; Nakatani, K.; Journaux, Y. *Mol. Cryst. Liq. Cryst.* **1989**, *176*, 481.

(17) Caneschi, A.; Gatteschi, D.; Sessoli, R. *Acc. Chem. Res.* **1989**, *22*, 392 and references therein.

(18) (a) Iwamura, H. *Pure Appl. Chem.* **1987**, *59*, 1595 and references therein. (b) Iwamura, H. *Pure Appl. Chem.* **1986**, *58*, 187 and references therein.

(19) (a) Itoh, K.; Takui, T.; Teki, Y.; Kinoshita, T. *J. Mol. Electron.* **1988**, *4*, 181. (b) Fujita, I.; Teki, Y.; Takui, T.; Kinoshita, T.; Itoh, K. *J. Am. Chem. Soc.* **1990**, *112*, 4074.

(20) Dougherty, D. A. *Pure Appl. Chem.* **1990**, *62*, 519.

(21) Caneschi, A.; Gatteschi, D.; Laugier, J.; Rey, P.; Sessoli, R.; Zanchini, C. *J. Am. Chem. Soc.* **1988**, *110*, 2795.

(22) McCusker, J. K.; Schmitt, E. A.; Hendrickson, D. N. High Spin Inorganic Clusters: Spin Frustration in Polynuclear Iron and Manganese Complexes. In ref 14.

(23) Farneth, W. E.; McLean, R. S.; McCarron, E. M.; Zuo, F.; Lu, Y.; Patton, B. R.; Epstein, A. J. *Phys. Rev. B: Condens. Matter* **1989**, *39*, 6594.

(24) Ghose, S.; Hewat, A. W.; Pinkney, M. *Solid State Commun.* **1990**, *74*, 413.

6116 *J. Am. Chem. Soc., Vol. 113, No. 16, 1991*

McCusker et al.

Table I. Analytical Data for Magnetic Samples

sample			% C	% H	% N	% Fe
a	$3 \cdot 1/2 CH_2Cl_2$	calc	33.68	4.12	7.76	
		found	33.66	4.22	7.79	
b	$3 \cdot 3/4 CH_2Cl_2$	calc	33.39	4.09	7.64	
		found	33.40	4.19	7.39	
c	$3 \cdot CH_2Cl_2$	calc	33.12	4.07	7.54	22.53
		found	33.12	4.16	7.61	22.54
d	$3 \cdot 3/4 CH_3CN \cdot 3/2 CH_2Cl_2$	calc	33.10	4.09	7.86	21.48
		found	33.05	4.33	7.75	21.40
e	$3 \cdot 1/2 CH_3CN \cdot 3/2 CH_2Cl_2$	calc	32.93	4.06	7.68	21.62
		found	31.10	3.73	8.30	21.67
f	$3 \cdot 3/4 CH_2Cl_2$	calc	33.39	4.09	7.64	22.86
		found	31.34	3.62	7.66	22.81

g, 60% yield). Mp: 167–169 °C. IR (cm^{-1}): 3108 (s), 2993 (s), 2945 (m), 2856 (m), 2796 (m), 1542 (w), 1523 (m), 1488 (s), 1438 (m), 1402 (m), 1388 (m), 1366 (m), 1341 (m), 1284 (s), 1233 (m), 1204 (m), 1157 (m), 1146 (m), 1109 (s), 1095 (m), 1080 (s), 1043 (w), 933 (s), 846 (w), 816 (m), 800 (m), 774 (s), 753 (s), 735 (s), 695 (s). ^{1}H NMR (300 MHz, CDCl$_3$): δ 2.04 (s, 3 H), 3.27 (s, 6 H), 5.46 (s, br, 1 H), 6.80 (s, 2 H), 6.95 (s, 2 H). ^{13}C NMR (75 MHz, CDCl$_3$): δ 27.78, 33.34, 69.36, 123.27, 125.86, 148.63. LRMS EI *m/e* (%): 206 (9), 205 (7), 192 (10), 191 (88), 163 (22), 125 (26), 109 (100), 107 (29), 96 (19), 95 (14), 83 (46), 82 (24), 81 (21), 54 (9), 42 (11). Anal. Calcd for C$_{10}$H$_{14}$N$_4$O: C, 58.24; H, 6.84; N, 27.17. Found: C, 58.37; H, 6.94; N, 27.32.

[Fe$_3$O(OAc)$_6$(py)$_3$](ClO$_4$) (2). Complex 2 was prepared by a modification of the procedure of Uemura et al.[25] To a stirred slurry of FeCl$_3$·6H$_2$O (5.95 g, 22 mmol) in ethanol (100 mL) and pyridine (20 mL) was added NaOAc (6.26 g, 46 mmol). After 30 min, NaCl was removed via filtration. Subsequent addition of NaClO$_4$ (1.22 g, 10 mmol) to this homogeneous solution gave a green precipitate, which was filtered out and recrystallized from CH$_2$Cl$_2$ to give complex 2·3H$_2$O (2.86 g, 42% yield). Anal. Calcd for 2·3H$_2$O (Fe$_3$O$_{20}$C$_{27}$H$_{39}$N$_3$Cl): C, 34.92; H, 4.23; N, 4.53. Found: C, 34.99; H, 4.12; N, 4.69.

[Fe$_6$O$_2$(OH)$_2$(OAc)$_{10}$(C$_{10}$H$_{13}$N$_4$O)$_2$] (3). Hydroxy diimidazole 1 (0.40 g, 1.94 mmol) was added to a stirred solution of complex 2 (0.56 g, 0.64 mmol) in MeCN (60 mL) to give a dark brown solution. After 20 min, the reaction mixture was concentrated in vacuo to give a brown oil (concentration to dryness did not affect yield or purity of product). This oil was dissolved in CH$_2$Cl$_2$ and the resulting solution allowed to slowly concentrate at room temperature. Crystals of complex 3 were isolated and dried in vacuo to give 3·CH$_2$Cl$_2$ (0.19 g, 40% yield). IR (cm^{-1}): 3434 (br), 3128 (w), 2994 (w), 2944 (w), 1571 (s), 1492 (m), 1428 (s), 1347 (m), 1286 (w), 1230 (w), 1214 (w), 1168 (w), 1152 (w), 1115 (m), 1088 (m), 1047 (w), 1025 (m), 935 (m), 746 (w), 657 (m). Anal. Calcd for 3·CH$_2$Cl$_2$ (Fe$_6$O$_{26}$C$_{41}$H$_{60}$N$_8$Cl$_2$): C, 33.12; H, 4.07; N, 7.54; Fe, 22.53. Found: C, 33.12; H, 4.16; N, 7.61; Fe, 22.54. Electronic spectrum (MeCN) [λ$_{max}$, nm (ε$_M$/Fe, cm^{-1} M^{-1})]: 463 (197), 325 (2205), 237 (5161). Mp: 230 °C dec.

Several samples of complex 3 were independently prepared to check the reproducibility of the magnetic susceptibility data. The specific conditions under which each sample was isolated are described below. Samples a–c were prepared from the reaction of complex 2 with hydroxy diimidazole 1 in MeCN as described above and concentrated in vacuo. For sample a, the resulting oil was dissolved in reagent grade CH$_2$Cl$_2$, and the solution was allowed to slowly concentrate for 1 week at room temperature. The crystals were then dried in an Abderhalden flask over refluxing acetone for 48 h. For sample b, the resulting oil was dissolved in dry CH$_2$Cl$_2$ (distilled from CaH$_2$). Crystals formed during 7 days of slow evaporation of the solvent. The crystals were then dried in an Abderhalden flask over refluxing acetone for 10 h. For sample c, the resulting oil was dissolved in dry CH$_2$Cl$_2$, and the solution was allowed to slowly concentrate. After 7 days, crystals were isolated and stored in 2:3 (v/v) CH$_2$Cl$_2$/hexane for ca. 2 months. The sample was then dried by filtration.

Samples d–f were prepared independently from the reaction of [Fe$_3$-(OAc)$_6$(H$_2$O)$_3$]NO$_3$[26] with hydroxy diimidazole 1 in MeCN. Each solution was concentrated in vacuo to give an oil, which was dissolved in dry CH$_2$Cl$_2$. Evaporation of solvent gave crystals in 3 days. Each sample was dried by filtration. Elemental analyses of samples e and f indicated the presence of an impurity, possibly due to nitrate being present. Analytical data for these samples are presented in Table I.

Table II. Crystallographic Data for
[Fe$_6$O$_2$(OH)$_2$(OAc)$_{10}$(C$_{10}$H$_{13}$N$_4$O)$_2$]·8CH$_2$Cl$_2$

formula	C$_{48}$H$_{74}$N$_8$O$_{26}$Cl$_{16}$Fe$_6$
M_r	2081.4
color, habit	red, block
cryst dimens, mm	0.41 × 0.55 × 0.83
cryst system	triclinic
space group	$P\bar{1}$ (No. 2, C_i^1)
temp, °C	–100
a, Å	12.167 (2)
b, Å	12.921 (4)
c, Å	15.394 (4)
α, deg	114.41 (2)
β, deg	97.641 (15)
γ, deg	102.17 (2)
V, Å^3	2087.4 (8)
Z	1
D(calc), g/cm^3	1.656
abs coeff, mm^{-1}	1.603
radiation type (λ, Å)	Mo Kα (0.710 73)
goodness of fit $(S)^a$	2.25
2θ range, deg	$4.0 \leq 2\theta \leq 45.0$
octants collected	$\pm h, \pm k, \pm l$
no. of total data	5498
no. of unique data	5363
no. of obsd data	4179, $F > 6.0\sigma(F)$
$R(F)$, %^{b}	4.65
$R_w(F)$, %^{c,d}	5.91

$^a S = [\sum_w(|F_o| - |F_c|)^2/(m - n)]^{1/2}$. $^b R = \sum(||F_o| - |F_c||)/\sum|F_o|$. $^c R_w = [(|F_o| - |F_c|)^2/\sum|F_o|^2]^{1/2}$. $^d w^{-1} = \sigma^2(F) + 0.0004F^2$.

X-ray Crystallography. Crystals were grown by slow evaporation of a solution of complex 3 in CH$_2$Cl$_2$ at room temperature. Since solvent loss was rapid, the crystal was covered with a thin layer of epoxy resin and mounted on a glass fiber. Data were collected at approximately –100 °C on a Siemens R3m/V automated four-circle diffractometer equipped with a graphite crystal monochromator employing the 2θ–θ scan method. The structure of complex 3 was solved by direct methods (SHELXTL PLUS) and refined by the full-matrix least-squares method with scattering factors taken from Cromer and Waber.[27] A summary of crystallographic data is given in Table II. The cell parameters were obtained from 24 reflections in the range 15° < 2θ < 30°. A systematic search of a full hemisphere of reciprocal space located a set of diffraction maxima with no symmetry or systematic absences, indicating a triclinic space group. Subsequent solution and refinement confirmed the centrosymmetric space group $P\bar{1}$. Three standard reflections were monitored after every 100 reflections. Intensities of these reflections decreased by ca. 6% during 65 h of X-ray exposure; an appropriate scale factor was applied to account for the decay. All non-hydrogen atoms were refined anisotropically. Hydrogen atoms were included in ideal positions by using the Riding model with *U* fixed at 0.08 Å^2. Eight solvent molecules (CH$_2$Cl$_2$) were found in the unit cell. There was evidence that two of the chlorine atoms (Cl(5) and Cl(7)) were disordered. Two different positions for both of these chlorine atoms were refined with fractional occupancies of 0.50. No absorption correction was applied. Final positional parameters are given in Table III.

Physical Measurements. Infrared spectra were collected on a Mattson Galaxy Model 2020 FTIR spectrophotometer as KBr pellets. Electronic spectra were measured by a Hewlett Packard Model 8452A diode array spectrophotometer. Each spectrum represents a signal average of 250 spectra taken at 0.1-s intervals. Temperature control was achieved by using a Hewlett Packard Model 89054A thermostated cell holder connected to a Fisher Scientific Isotemp Model 800 circulating bath. The temperature was maintained at 30.0 ± 0.3 °C; the absolute accuracy is estimated to be ±1 °C. ^{1}H and ^{13}C NMR spectra were collected at ambient temperature on a General Electric QE 300 NMR spectrometer.

Magnetic measurements of complex 3·CH$_2$Cl$_2$ were carried out by using a VTS Model 900 SQUID magnetometer (BTi, Inc., San Diego, CA). Bulk susceptibility data were collected on finely ground samples in an applied field of 10.00 kG between 6 and 350 K. Variable-field magnetization data were collected on complex 3·CH$_2$Cl$_2$ immersed in a petroleum gel mull to prevent torquing of the crystallites at high fields. Data were collected as a function of temperature in applied fields of 10.00 kG (1.51–9.04 K), 25.00 kG (1.81–9.00 K), and 40.00 kG (1.57–9.04 K). In none of the data was there any evidence of texturing due to field-induced polarization of the crystallites. The mass of the magnetization

(25) Uemura, S.; Spencer, A.; Wilkinson, G. *J. Chem. Soc., Dalton Trans.* **1973**, 2565.

(26) Johnson, M. K.; Powell, D. B.; Cannon, R. D. *Spectrochim. Acta* **1981**, *37A*, 995.

(27) Cromer, D. T.; Waber, J. T. *International Tables for X-ray Crystallography*; Kynoch Press: Birmingham, England, 1974; Vol. IV, Table 2.2A.
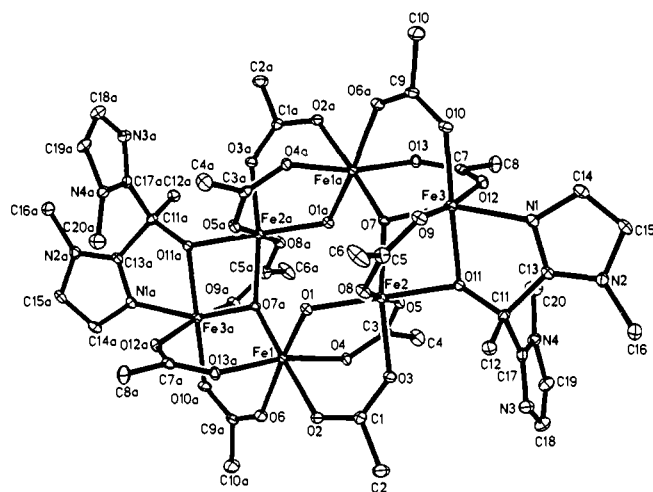
Figure 1. ORTEP drawing of the Fe$^{III}_6$ complex [Fe$_6$O$_2$(OH)$_2$(OAc)$_{10}$-(C$_{10}$H$_{13}$N$_4$O)$_2$]·8CH$_2$Cl$_2$. Solvent molecules have been omitted for clarity.

sample was calculated on the basis of the previously determined gram susceptibility of complex **3** at 10.00 kG for $T = 6.00$ K and $T = 8.00$ K. Diamagnetic corrections were applied to all of the data by use of Pascal's constants.[28]

Results and Discussion

Synthesis. The hexanuclear ferric complex **3** was prepared by the addition of hydroxy diimidazole **1** to a solution of trinuclear complex **2** in acetonitrile. Concentration in vacuo gave a brown
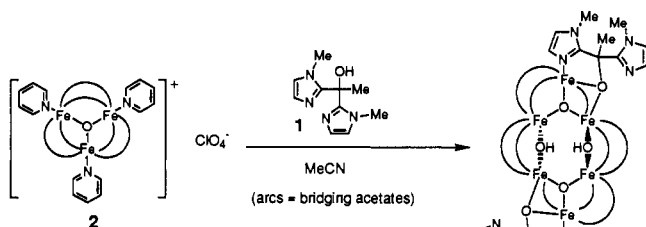
oil that was soluble in a variety of solvents including CH$_2$Cl$_2$, CHCl$_3$, MeCN, and acetone. Recrystallization by slow evaporation of a CH$_2$Cl$_2$ solution of this brown oil gave block crystals of complex **3**. From X-ray crystallography it was determined that eight CH$_2$Cl$_2$ molecules were present per molecule of **3**. Due to solvent loss, exposure to air caused a loss of crystallinity. If stored in solvent (CH$_2$Cl$_2$/hexanes (2:3, v/v)) the crystals remained stable. Upon drying in vacuo at 56 °C, only one solvent molecule per molecule of **3** remained, as determined by elemental analysis. Crystals dried by filtration in air left two to four solvent molecules per molecule of **3**. It was also found that other iron triangles, such as [Fe$_3$O(OAc)$_6$(H$_2$O)$_3$]NO$_3$, could be used in an analogous reaction to give the same hexanuclear complex **3**.

The samples that were used for the magnetic studies were made from independently prepared samples of starting iron triangles. To check the reproducibility of the magnetic susceptibility data, a variety of samples were studied. The conditions for crystal growth were varied to determine if there were any changes in the magnetic data due to iron oxide impurities. It can be seen from Table I that different preparations do yield the same formulation of complex **3** with only slight variations in the degree of solvation. The variation in composition had no effect on the magnetic properties of the complex (vide infra).

Description of Structure. An ORTEP drawing of complex **3** is shown in Figure 1. A stereoview of complex **3** is available in the supplementary material. Selected structural parameters are listed in Table IV. Complex **3** crystallizes in the triclinic space group

(28) *Theory and Applications of Molecular Paramagnetism*; Boudreaux, E. A., Mulay, L. N., Eds.; John Wiley and Sons, Inc.: New York, 1976.

Table III. Positional and Equivalent Isotropic Thermal Parameters for [Fe$_6$O$_2$(OH)$_2$(OAc)$_{10}$(C$_{10}$H$_{13}$N$_4$O)$_2$]·8CH$_2$Cl$_2$

atom	x/a	y/b	z/c	U(eq), $\text{Å}^2 \times 10^3$
Fe(1)	0.6319 (1)	0.6374 (1)	0.1801 (1)	18 (1)
Fe(2)	0.5719 (1)	0.6525 (1)	−0.0396 (1)	18 (1)
Fe(3)	0.4667 (1)	0.5613 (1)	−0.2524 (1)	19 (1)
O(1)	0.5244 (3)	0.6365 (3)	0.0714 (3)	19 (2)
O(2)	0.7241 (3)	0.8085 (3)	0.2088 (3)	26 (2)
O(3)	0.7032 (3)	0.7950 (3)	0.0570 (3)	25 (2)
O(4)	0.7517 (3)	0.5848 (3)	0.1057 (3)	23 (2)
O(5)	0.6778 (3)	0.5436 (3)	−0.0499 (3)	22 (2)
O(6)	0.7526 (3)	0.6683 (4)	0.3029 (3)	28 (2)
O(7)	0.4523 (3)	0.5177 (3)	−0.1493 (3)	18 (2)
O(8)	0.4666 (3)	0.7591 (3)	−0.0333 (3)	25 (2)
O(9)	0.3868 (3)	0.6906 (3)	−0.1954 (3)	26 (2)
O(10)	0.3122 (3)	0.4704 (3)	−0.3505 (3)	26 (2)
O(11)	0.6183 (3)	0.6713 (3)	−0.1542 (3)	20 (2)
O(12)	0.5237 (3)	0.4195 (3)	−0.3288 (3)	24 (2)
O(13)	0.4600 (3)	0.2835 (3)	−0.2773 (3)	24 (2)
N(1)	0.5454 (4)	0.6490 (4)	−0.3274 (3)	22 (2)
N(2)	0.6985 (4)	0.7702 (4)	−0.3317 (4)	28 (2)
N(3)	0.8961 (5)	0.8691 (5)	−0.0723 (4)	33 (2)
N(4)	0.8606 (4)	0.6776 (4)	−0.1733 (4)	28 (2)
C(1)	0.7439 (5)	0.8505 (5)	0.1498 (4)	22 (3)
C(2)	0.8213 (6)	0.9749 (6)	0.1900 (5)	37 (3)
C(3)	0.7519 (5)	0.5431 (5)	0.0163 (4)	22 (3)
C(4)	0.8460 (6)	0.4889 (7)	−0.0153 (5)	41 (3)
C(5)	0.3976 (5)	0.7566 (5)	−0.1040 (5)	28 (3)
C(6)	0.3243 (7)	0.8398 (7)	−0.0791 (5)	51 (4)
C(7)	0.5187 (5)	0.3232 (5)	−0.3245 (4)	23 (3)
C(8)	0.5885 (6)	0.2474 (6)	−0.3814 (5)	37 (3)
C(9)	0.2367 (5)	0.3817 (5)	−0.3569 (4)	25 (3)
C(10)	0.1272 (6)	0.3330 (7)	−0.4365 (5)	43 (3)
C(11)	0.6904 (5)	0.7635 (5)	−0.1676 (4)	21 (3)
C(12)	0.6717 (5)	0.8839 (5)	−0.1094 (4)	27 (3)
C(13)	0.6488 (5)	0.7269 (5)	−0.2768 (4)	22 (3)
C(14)	0.5283 (6)	0.6435 (5)	−0.4206 (4)	27 (3)
C(15)	0.6219 (6)	0.7166 (6)	−0.4246 (4)	32 (3)
C(16)	0.8120 (6)	0.8592 (7)	−0.3017 (5)	45 (4)
C(17)	0.8175 (5)	0.7711 (5)	−0.1367 (4)	25 (3)
C(18)	0.9972 (6)	0.8375 (6)	−0.0657 (5)	40 (3)
C(19)	0.9773 (5)	0.7212 (6)	−0.1251 (5)	36 (3)
C(20)	0.7990 (6)	0.5547 (6)	−0.2455 (5)	39 (3)
Cl(1)	0.0675 (2)	0.6730 (2)	0.2606 (2)	75 (1)
Cl(2)	0.0171 (2)	0.8009 (2)	0.1505 (2)	56 (1)
Cl(3)	0.5294 (2)	1.0522 (2)	0.2902 (2)	74 (1)
Cl(4)	0.3189 (2)	0.8563 (2)	0.1845 (2)	57 (1)
Cl(5A)	0.8430 (4)	0.1050 (4)	0.4582 (3)	71 (1)
Cl(5B)	0.9183 (4)	0.0003 (4)	0.4687 (4)	74 (1)
Cl(6)	0.7050 (2)	−0.0178 (2)	0.5355 (2)	77 (1)
Cl(7A)	0.8169 (3)	0.4071 (4)	0.5089 (3)	56 (1)
Cl(7B)	0.8065 (5)	0.3111 (5)	0.4856 (4)	82 (1)
Cl(8)	0.9186 (2)	0.3235 (3)	0.3379 (2)	89 (2)
C(21)	0.0035 (6)	0.7801 (6)	0.2553 (5)	44 (3)
C(22)	0.4692 (6)	0.9033 (6)	0.2006 (5)	42 (3)
C(23)	0.7564 (8)	−0.0221 (8)	0.4351 (5)	63 (4)
C(24)	0.7941 (8)	0.3258 (8)	0.3815 (6)	61 (4)

$P\bar{1}$. The complex possesses an imposed C_i symmetry and therefore has three unique Fe^{III} ions.

The complex as a whole contains six iron atoms arranged in a planar configuration (the maximum deviation of an iron atom is 0.04 (1) Å). The μ_2-hydroxide oxygen atom O(1a) is bridging below this plane (0.82 (1) Å), while the symmetry-related atom O(1) is above the Fe$_6$ plane. The μ_3-oxo atoms O(7) and O(7a) are 0.18 (1) Å below and above the plane, respectively. The bridging alkoxide oxygen O(11) and the terminal imidazole nitrogen N(1) from the hydroxy diimidazole ligand **1** are both above the plane by 0.72 (1) and 0.59 (1) Å, respectively, while the symmetry-related atoms O(11a) and N(1a) are below the Fe$_6$ plane by the corresponding distances.

The structure of complex **3** may be viewed as two Fe$^{III}_3$ μ_3-oxo complexes. Fe(1) and Fe(2a) in one triangle are bridged to the corresponding edge atoms, Fe(2) and Fe(1a), of the other triangle and are held together by two μ_2-hydroxo and four bridging acetato ligands. The μ_3-oxo atom O(7) is 0.16 (1) Å below the plane

Table IV. Selected Distances (Å) and Angles (deg) for
$[Fe_6O_2(OH)_2(OAc)_{10}(C_{10}H_{13}N_4O)_2]\cdot 8CH_2Cl_2$

Distances			
Fe(1)-O(1)	1.977 (4)	Fe(3)-O(7)	1.908 (5)
Fe(1)-O(2)	2.087 (4)	Fe(3)-O(9)	2.051 (5)
Fe(1)-O(4)	2.029 (4)	Fe(3)-O(10)	2.011 (3)
Fe(1)-O(6)	2.069 (4)	Fe(3)-O(11)	2.021 (3)
Fe(1)-O(7a)	1.873 (4)	Fe(3)-O(12)	2.048 (4)
Fe(1)-O(13a)	2.048 (4)	Fe(3)-N(1)	2.111 (6)
Fe(2)-O(1)	1.948 (4)	Fe(2)···Fe(3)	2.970 (1)
Fe(2)-O(3)	2.004 (3)	Fe(1a)···Fe(2)	3.580 (1)
Fe(2)-O(5)	2.074 (5)	Fe(1a)···Fe(3)	3.269 (1)
Fe(2)-O(7)	1.963 (3)	Fe(1)···Fe(2)	3.458 (1)
Fe(2)-O(8)	2.053 (5)		
Fe(2)-O(11)	2.014 (5)		

Angles			
O(1)-Fe(1)-O(2)	86.7 (2)	O(2)-Fe(1)-O(4)	85.1 (2)
O(1)-Fe(1)-O(4)	97.4 (2)	O(2)-Fe(1)-O(6)	84.4 (2)
O(1)-Fe(1)-O(6)	170.6 (2)	O(2)-Fe(1)-O(7a)	177.8 (2)
O(1)-Fe(1)-O(7a)	91.5 (2)	O(2)-Fe(1)-O(13a)	86.9 (2)
O(1)-Fe(1)-O(13a)	90.7 (2)	O(6)-Fe(1)-O(7a)	97.4 (2)
O(4)-Fe(1)-O(6)	84.9 (2)	O(6)-Fe(1)-O(13a)	85.8 (2)
O(4)-Fe(1)-O(7a)	94.0 (2)	O(7a)-Fe(1)-O(13a)	94.3 (2)
O(4)-Fe(1)-O(13a)	168.2 (1)	O(3)-Fe(2)-O(5)	90.4 (2)
O(1)-Fe(2)-O(3)	88.4 (2)	O(3)-Fe(2)-O(7)	171.4 (2)
O(1)-Fe(2)-O(5)	92.4 (2)	O(3)-Fe(2)-O(8)	90.3 (2)
O(1)-Fe(2)-O(7)	100.2 (2)	O(3)-Fe(2)-O(11)	91.7 (2)
O(1)-Fe(2)-O(8)	89.1 (2)	O(7)-Fe(2)-O(8)	89.8 (2)
O(1)-Fe(2)-O(11)	178.7 (2)	O(7)-Fe(2)-O(11)	79.7 (2)
O(5)-Fe(2)-O(7)	89.3 (2)	O(8)-Fe(2)-O(11)	89.6 (2)
O(5)-Fe(2)-O(8)	178.4 (2)	O(9)-Fe(3)-O(10)	83.7 (2)
O(5)-Fe(2)-O(11)	89.0 (2)	O(9)-Fe(3)-O(11)	90.4 (1)
O(7)-Fe(3)-O(9)	91.4 (2)	O(9)-Fe(3)-O(12)	170.6 (1)
O(7)-Fe(3)-O(10)	103.4 (2)	O(9)-Fe(3)-N(1)	90.4 (2)
O(7)-Fe(3)-O(11)	80.9 (2)	O(11)-Fe(3)-O(12)	98.5 (2)
O(7)-Fe(3)-O(12)	92.7 (2)	O(11)-Fe(3)-N(1)	76.9 (2)
O(7)-Fe(3)-N(1)	157.7 (1)	O(12)-Fe(3)-N(1)	88.9 (2)
O(10)-Fe(3)-O(11)	172.7 (2)	Fe(2)-O(7)-Fe(1a)	137.9 (3)
O(10)-Fe(3)-O(12)	87.2 (2)	Fe(2)-O(7)-Fe(3)	100.2 (2)
O(10)-Fe(3)-N(1)	98.8 (2)	Fe(3)-O(7)-Fe(1a)	119.7 (2)
Fe(1)-O(1)-Fe(2)	123.5 (2)		
Fe(2)-O(11)-Fe(3)	94.8 (2)		

defined by the three iron atoms Fe(1a), Fe(2), and Fe(3). The three Fe···Fe distances within these triangular subunits are inequivalent (Fe(1a)···Fe(2) = 3.580 (1) Å, Fe(1a)···Fe(3) = 3.269 (1) Å, Fe(2)···Fe(3) = 2.970 (1) Å), thus giving a scalene triangle. One edge of the triangle [Fe(1a), Fe(3)] is metrically very similar to those typically found in μ_3-oxo-bridged Fe^{III}_3 equilateral triangles.[29] Fe(1a) and Fe(3) are bridged by two bidentate acetate groups with a Fe(3)-O(7)-Fe(1a) angle of 119.7 (2)°. The second edge [Fe(2), Fe(3)] of this same triangle is bridged by the deprotonated alkoxide oxygen O(11) and one bridging acetate group. The Fe(3)-O(11)-Fe(2) angle is quite small, 94.8 (2)°, resulting in a reduced distance (2.970 (1) Å) between the iron centers, Fe(2) and Fe(3). The Fe(2)-O(7)-Fe(3) angle of 100.2 (2)° is significantly smaller than the other two Fe-O(7)-Fe angles. The third edge of this triangle [Fe(1a), Fe(2)] is longer than the other two edges. These two iron ions are bridged by only the μ_3-O(7), thus giving a longer Fe···Fe distance of 3.580 (1) Å with an Fe(1a)-O(7)-Fe(2) angle of 137.9 (3)°. The distance between the two triangular complexes Fe(1)···Fe(2) is 3.458 (1) Å. This distance is shorter than the longest edge [Fe(1), Fe(2a)] of each triangular subunit.

Iron atoms Fe(1) and Fe(2) both have only oxygen ligation whereas Fe(3) has both oxygen and nitrogen ligation. Fe(1) is bound to one μ_3-oxo (1.873 (4) Å), one μ_2-hydroxo (1.977 (4) Å), and four acetate oxygen atoms. Fe(2) has the same coordination as Fe(1) [one μ_3-oxo (1.963 (3) Å), one μ_2-hydroxo (1.948 (4) Å)] with the exception that one of the acetate oxygens is replaced by a μ_2-alkoxide (2.014 (5) Å) from hydroxy diimidazole 1. Fe(3),

like Fe(2), has only three μ_2-acetato oxygen atoms in its coordination sphere in addition to the μ_3-oxo (1.908 (5) Å). The remaining coordination sites of Fe(3) are occupied by a nitrogen atom of one of the imidazoles (2.111 (6) Å) of 1 and the μ_2-alkoxide (2.021 (3) Å) from 1. The second imidazole ring of 1 is not bound to any of the iron centers. This type of bonding has been seen previously in a trinuclear iron–oxo complex.[30] The metal–ligand bond distances of 3 are typical for high-spin Fe^{III} complexes. However, it is important to note that all of the Fe–μ_3-O(7) distances are distinctly different: Fe(3), 1.908 (5) Å; Fe(2), 1.963 (3) Å; Fe(1a), 1.873 (4) Å. All of the iron atoms are in a pseudooctahedral environment in complex 3 with the coordination geometry of Fe(3) being somewhat distorted due to the bite angle of the hydroxy diimidazole ligand 1 [O(11)-Fe-(3)-N(1) angle is only 76.9 (2)°].

Three other hexanuclear Fe^{III} complexes have been reported.[6d-h] Complex 3 is similar to $Fe_6O_2(OH)_2(O_2CCMe_3)_{12}$ (4)[6d,e] but is quite different from $Fe_6O_2(OH)_2(O_2CPh)_{12}(1,4\text{-dioxane})(OH_2)$ (5).[6f] See Table V for a comparison of selected structural features of 3 to those of 4 and 5.
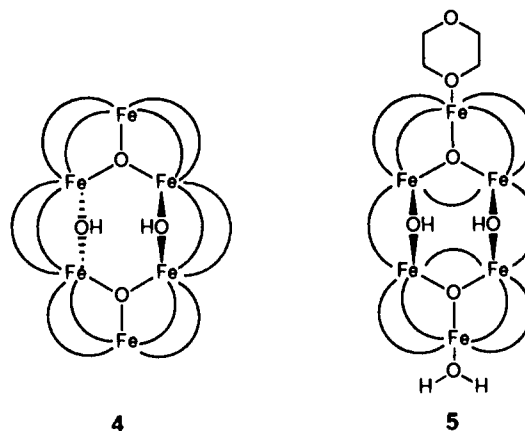
4
(arcs = bridging pivalates)

5
(arcs = bridging benzoates)

As with complex 3, the six iron atoms of complex 4 are roughly planar with one μ_2-hydroxo group bridging above the plane and one μ_2-hydroxo group bridging below the plane. Both complexes have similar Fe–μ_2-OH bond distances: 1.98 and 1.96 Å for complex 4; 1.977 (4) and 1.948 (4) Å for 3. The Fe–μ_2-OH–Fe angles are also comparable: 122.2° in 4 and 123.5 (2)° in 3. Four carboxylato (pivalato) ligands are also bridging between the two edge-facing triangular subunits. The separations of the two triangular subunits are nearly identical in 3 and 4: 3.458 (1) Å in the former and 3.45 Å in the latter.

The primary differences between 3 and 4 occur in the symmetry of the trinuclear subunits. Due to the nature in which the hydroxy diimidazole ligand 1 binds in complex 3, the triangular subunit is asymmetric. In 3, the exterior edge of the triangle with the μ_2-alkoxo group has an Fe···Fe distance of 2.970 (1) Å. The other exterior edge of 3 has an Fe···Fe distance of 3.269 (1) Å. In complex 4, the two exterior edges of the triangle have the same environment, resulting in a more symmetrical structure (Fe···Fe = 3.13 and 3.17 Å). In both 4 and 3, the interior edge is only bridged by the μ_3-oxo atom. The Fe···Fe distance is distinctly longer along this interior edge (3.45 Å in 4 and 3.458 (1) Å in 3). The symmetry difference between complexes 3 and 4 is also seen in the three μ_3-O-Fe bond lengths: 1.85, 1.94, and 1.94 Å in 4; 1.873 (4), 1.908 (5), and 1.963 (3) Å in 3. In 4, all of the iron coordination is via oxygen atoms with the apical iron atoms being five-coordinate.

The iron atoms in complex 5 also contain only oxygen in the coordination spheres. The six iron atoms in 5, however, form a twisted-boat conformation instead of the planar conformation found in both 3 and 4. The four central iron atoms form a distorted plane in complex 5 with the two apical iron atoms both

(29) (a) Blake, A. B.; Fraser, L. R. *J. Chem. Soc., Dalton Trans.* **1975,** 193. (b) Azenhofer, K.; De Boer, J. J. *Recl. Trav. Chim. Pays-Bas* **1969,** *88,* 286.

(30) Gorun, S. M.; Papaefthymiou, G. C.; Frankel, R. B.; Lippard, S. J. *J. Am. Chem. Soc.* **1987,** *109,* 4244.

Table V. Structural Comparisons of the Hexanuclear Complexes

property	3[a]	4[b]	5[c]
Fe···Fe, Å (in triangular subunit)	2.970, 3.580, 3.269	3.13, 3.59, 3.17	3.30, 3.43, 3.29, 3.30, 3.43, 3.28
Fe···Fe, Å (between subunits)	3.458	3.45	3.64, 3.62
Fe–μ_2–OH, Å	1.977, 1.948	1.98, 1.96	2.000, 2.003, 1.962, 1.985
Fe–μ_3–O, Å	1.873, 1.963, 1.908	1.85, 1.94, 1.94	1.943, 1.869, 1.971, 1.950, 1.871, 1.965
Fe–μ_2–OH–Fe, deg	123.5	122.2	129.9, 134.4
Fe–μ_3–O–Fe, deg	137.9, 119.7, 100.2	135.2, 113.5, 111.2	118.7, 118.9, 122.4, 122.3, 119.7, 117.9
space group	$P\bar{1}$	$P\bar{1}$	$P2_1/n$
rel position of μ_2–OH	opposite sides of Fe$_4$ plane	opposite sides of Fe$_4$ plane	same side of Fe$_4$ plane
geometry	planar	planar	twisted boat

[a] This work. [b] Reference 6d. [c] Reference 6e.

Table VI. Mössbauer Fitting Parameters for [Fe$_6$O$_2$(OH)$_2$(OAc)$_{10}$(C$_{10}$H$_{13}$N$_4$O)$_2$]

T, K	ΔE_Q, mm/s	δ,[a] mm/s	Γ,[b] mm/s	rel area
300	1.056 (11)	0.406 (6)	0.218 (9), 0.200 (4)	1
	0.729 (5)	0.383 (3)	0.199 (3), 0.250 (9)	2
200	1.061 (12)	0.510 (6)	0.239 (2), 0.239 (2)	1
	0.78 (3)	0.350 (14)	0.295 (7), 0.295 (7)	2

[a] Isomer shift relative to iron foil at room temperature. [b] Half-width at half-height taken from least-squares fitting program. The width for the line at more negative velocity is listed first for each doublet.

above the plane. As in 3 and 4, two μ_3-oxo Fe$^{III}_3$ subunits are bridged together. In 5, the ligation around the triangular subunits is different. The two Fe$_3$ μ_3-oxo subunits are still coupled by bridging hydroxides; however, both bridging hydroxides are on the same side of the distorted plane of the four central iron atoms. The Fe–μ_2-OH–Fe angles of the bridging hydroxides are larger in 5 (129.9 (4) and 134.4 (5)°) than in 3 (123.5 (2)°). Additionally, only two carboxylato (benzoato) ligands are bridging the two triangular subunits as opposed to four in complex 3. Complex 5 has a greater distance between the triangular subunits than 3: approximately 3.63 Å in the former and 3.458 (1) Å in the latter. Two additional carboxylates bridge along the edges of the trinuclear subunits that face one another.

When the triangular subunits of 5 and 3 are compared, many differences are apparent. In complex 3, the two subunits are symmetry related while in 5 they are not. However, each triangular subunit of 5 is more symmetrical than the triangular subunits of 3. This is best illustrated by comparison of the Fe···Fe distances (the edges of the triangle). The exterior edges in 5 are 3.29 and 3.30 Å (one subunit) and 3.28 and 3.30 Å (the other subunit) while the same edges in 3 are 2.970 (1) and 3.269 (1) Å. The short distance in 3 is a result of the bridging alkoxide. This difference in the symmetry of the triangular subunits is also reflected in the Fe–μ_3-O distances (see Table V). The interior edges (the edges of the triangular subunits facing one another) of 5 are not as long as the interior edge of 3: 3.43 Å for both interior edges in 5 and 3.580 (1) Å in 3.

The third hexanuclear complex, O[Fe(OCH$_2$)$_3$CCH$_3$]$_6$[N-(CH$_3$)$_4$]$_2$,[6h] is fundamentally different from 3–5. This complex possesses a μ_6-oxo atom octahedrally surrounded by six Fe(III) atoms. This OFe$_6$ core is surrounded by six deprotonated CH$_3$C(CH$_2$O)$_3^{3-}$ ligands. In addition to the μ_6-oxo atom, each distorted octahedral iron is bound to five alkoxide groups.

^{57}Fe Mössbauer Spectroscopy. Mössbauer spectra were run for a polycrystalline sample of complex 3 at 300, 200, and 100 K and are shown in Figure 2. These spectra are characteristic of high-spin Fe^{III} ions. The features in the 100 K spectrum are broad. It is not reasonable to fit this 100 K spectrum, for it is clear that it is affected by relaxation effects. The 200 and 300 K spectra could be fit with two Lorentzian line shapes characteristic of one quadrupole-split doublet; however, the line widths were large. Quite good fits of these two spectra could be obtained with two doublets in an area ratio of 2:1; see Figure 2. Least-squares fitting parameters are given in Table VI. The doublet with the larger area may be assigned to the Fe(1a) and Fe(2) atoms which have Fe^{III}O$_6$ environments, while the smaller doublet can be assigned to the Fe(3) atom which has a Fe^{III}O$_5$N environment. Preliminary experiments show that in the absence of
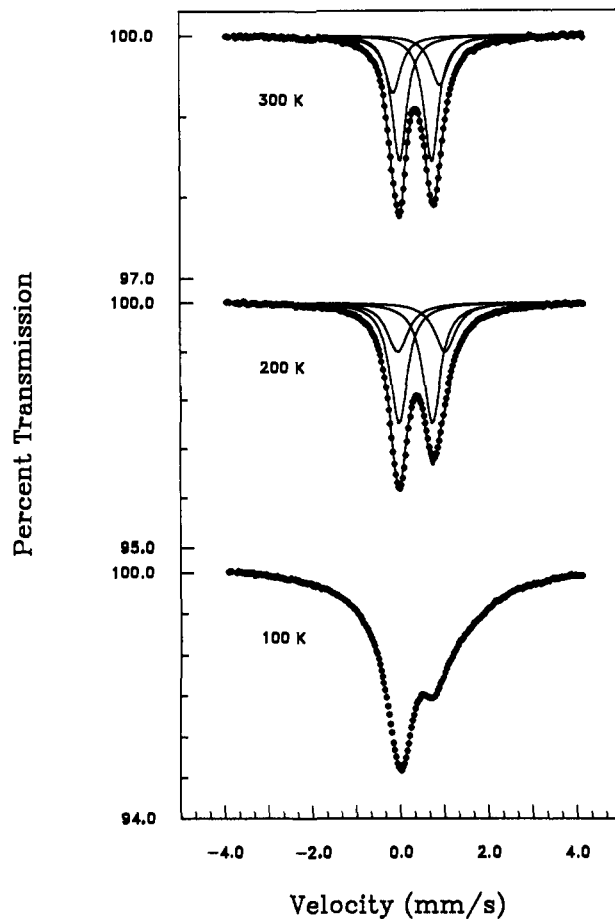
Figure 2. Variable-temperature ^{57}Fe Mössbauer spectra of [Fe$_6$O$_2$-(OH)$_2$(OAc)$_{10}$(C$_{10}$H$_{13}$N$_4$O)$_2$]·8CH$_2$Cl$_2$.

an external magnetic field, complex 3 at 4.2 K does *not* show hyperfine splitting in its Mössbauer spectrum.

Magnetochemistry. In Figure 3 is shown a plot of μ_{eff} per molecule versus temperature for complex 3·CH$_2$Cl$_2$ (sample c, Table I) in an applied field of 10.00 kG. The effective moment is 9.21 μ_B at 346.1 K, drops slightly to 9.06 μ_B at 278.7 K, and then rises gradually to a maximum of 10.90 μ_B at 20.00 K, where it plateaus before falling to 10.44 μ_B by 6.00 K. The overall profile of the curve, in particular the *increase* in effective moment with decreasing temperature, indicates an increase in average unpaired spin density at low temperature relative to that found at room temperature. This type of behavior is unprecedented for a discrete polynuclear Fe^{III} complex and strongly suggests that the ground state of complex 3 is *not* S = 0 but some larger value. The effective moment at 20.00 K is close to the spin-only value for a S = 5 state (μ_{eff} = 10.95 μ_B).

Since complex 3 is an all-ferric compound prepared from Fe^{III} starting materials, it was important to check that the magnetic behavior being observed is an intrinsic property of the molecule and not an artifact due to the presence of trace amounts of a highly magnetic oxide such as Fe$_2$O$_3$ or magnetite, Fe$_3$O$_4$. The presence of magnetite impurities could substantially affect magnetic data,
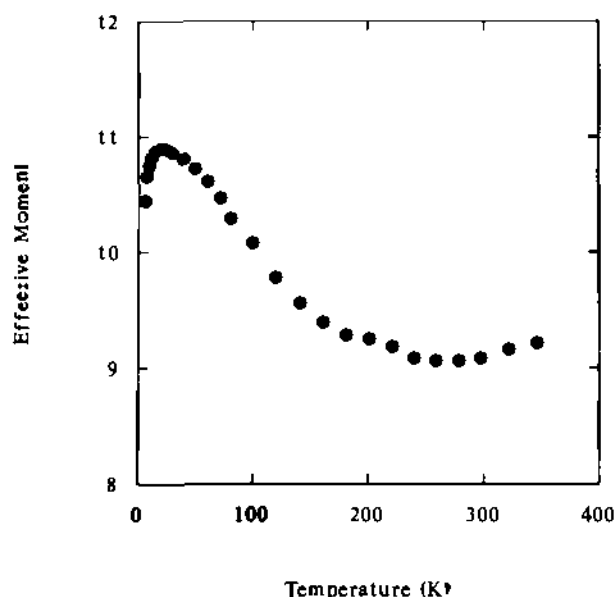
Temperature (K)

Figure 3. Plot of μ_{eff} versus temperature for {Fe$_6$O$_2$(OH)$_2$(OAc)$_{10}$-(C$_{10}$H$_{11}$N$_4$O)$_2$}·CH$_2$Cl$_2$ (3·CH$_2$Cl$_2$) in an applied field of 10.00 kG.

particularly at low temperatures. Figure 4 shows plots of effective moment versus temperature for four independently prepared samples (two different preparative procedures) in the temperature range 20–80 K. The data for samples e and f are not included, since we were unable to obtain satisfactory elemental analyses for these samples (vide supra). A table listing magnetic data for all six samples can be found in the supplementary material. It can be seen that the overall profile of the data remains consistent for all of the samples examined. In fact, the data for four of the samples essentially superimpose. The data for the two samples with the poorest analytical characterization (Table I, samples e and f) fall somewhat below the data for the other four samples. If the magnetic behavior of complex 3 were due to a ferromagnetic impurity, we would not anticipate that the impurity level would remain constant for six different preparations based on different starting materials. In addition, the fact that the more impure samples exhibit smaller moments implies that any impurities present are contributing to depress the moment. This is inconsistent with what one would expect if the impurity were ferromagnetic. In short, we are quite confident that the data in Figure 3 are indicative of a novel magnetic behavior for polynuclear Fe^{III} complex 3.

Theoretical Models. The complete spin Hamiltonian for complex 3, assuming each pairwise interaction is describable in terms of the Heisenberg Hamiltonian of the form $\hat{H} = -2J_{ij}\hat{S}_i\hat{S}_j$, is given by eq 1. In eq 1, we have adhered to the numbering scheme

$$\hat{H} = -2J_{12}\hat{S}_1\hat{S}_2 - 2J_{13}\hat{S}_1\hat{S}_3 - 2J_{14}\hat{S}_1\hat{S}_4 - 2J_{15}\hat{S}_1\hat{S}_5 - 2J_{16}\hat{S}_1\hat{S}_6 - 2J_{23}\hat{S}_2\hat{S}_3 - 2J_{24}\hat{S}_2\hat{S}_4 - 2J_{25}\hat{S}_2\hat{S}_5 - 2J_{26}\hat{S}_2\hat{S}_6 \quad (1)$$

indicated in Figure 1. By virtue of the crystallographically imposed inversion symmetry, eq 1 collapses directly to eq 2. The spin

$$\hat{H} = -2J_{12}(\hat{S}_1\hat{S}_2 + \hat{S}_1\hat{S}_2) - 2J_{13}(\hat{S}_1\hat{S}_3 + \hat{S}_2\hat{S}_3) - 2J_{14}(\hat{S}_1\hat{S}_4 + \hat{S}_2\hat{S}_4) - 2J_{15}(\hat{S}_1\hat{S}_5 + \hat{S}_1\hat{S}_6) \quad (2)$$

degeneracy of a hexanuclear high-spin Fe^{III} complex is 46 656. With the total spin of the system defined as $\hat{S}_T = \hat{S}_A + \hat{S}_{A'}$, where $\hat{S}_A = \hat{S}_1 + \hat{S}_2 + \hat{S}_3$ and $\hat{S}_{A'}$ is the inversion-related term, there are 4332 individual spin states. Among them are 111 states with $S_T = 0$ and 581 states with $S_T = 5$ arising from a wide range of vector-coupled combinations of (S_A, $S_{A'}$) terms. It now becomes clear, as was indicated above, why it is difficult to predict a priori which vector coupling might produce any particular ground state, including the $S = 0$ state observed for complex 5.

Our initial attempts to quantitatively analyze the variable-temperature susceptibility data collected at 10.00 kG focused on deriving an operator-equivalent expression for eq 2 by using the
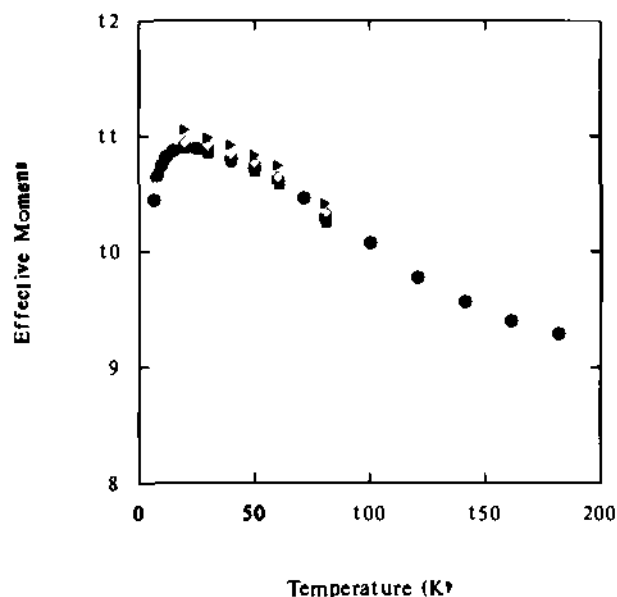
Temperature (K)

Figure 4. Plots of μ_{eff} versus temperature for independently prepared samples of {Fe$_6$O$_2$(OH)$_2$(OAc)$_{10}$(C$_{10}$H$_{11}$N$_4$O)$_2$}·xS: tilted triangles, sample a; tilted squares, sample b; circles, sample c, run 1; triangles, sample c, run 2; squares, sample d. See text for details regarding the exact composition of each sample.

Kambe vector-coupling approach.[31] However, it became clear that it is *not possible* to generate such an expression for complex 3 due to the topology, i.e., connectivity of the metal ions. The easiest way to understand this is to examine the situation that arises for a triangular arrangement of metal ions, such as is found for the {Fe$_3$O(O$_2$CR)$_6$L$_3$}$^+$ class of molecules. The pairwise interactions in such a system can be represented schematically as follows:
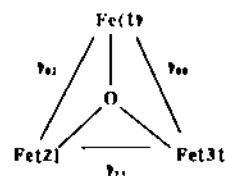
For the ease when all coupling pathways are equivalent, i.e., $J_{12} = J_{13} = J_{23}$, we can immediately write the spin Hamiltonian as

$$\hat{H} = -2J(\hat{S}_1\hat{S}_2 + \hat{S}_2\hat{S}_3 + \hat{S}_3\hat{S}_1) \quad (3)$$

If the total spin is defined as $\hat{S}_T = \hat{S}_1 + \hat{S}_2 + \hat{S}_3$, then an operator-equivalent expression for eq 3 can be readily generated

$$\hat{H} = -J(\hat{S}_T^2 - \hat{S}_1^2 - \hat{S}_2^2 - \hat{S}_3^2) \quad (4)$$

from which the corresponding eigenvalue equation can be obtained. Likewise, an isosceles topology is also handled by the Kambe coupling approach. For $J_{12} = J_{13}$, we may write the Hamiltonian as

$$\hat{H} = -2J(\hat{S}_1\hat{S}_2 + \hat{S}_1\hat{S}_3) - 2J_{23}(\hat{S}_2\hat{S}_3) \quad (5)$$

By defining $\hat{S}_T = \hat{S}_A + \hat{S}_1$, where $\hat{S}_A = \hat{S}_2 + \hat{S}_3$, the operator-equivalent form of eq 5 becomes

$$\hat{H} = -J(\hat{S}_T^2 - \hat{S}_A^2 - \hat{S}_1^2) - J_{23}(\hat{S}_A^2 - \hat{S}_2^2 - \hat{S}_3^2) \quad (6)$$

Again, an eigenvalue expression for this spin system can be written directly from eq 6. However, as Griffith has noted,[32] no such simple solution is obtainable for an asymmetric triangle, i.e., one in which $J_{12} \neq J_{13} \neq J_{23}$ and the Hamiltonian is

$$\hat{H} = -2J_{12}\hat{S}_1\hat{S}_2 - 2J_{13}\hat{S}_1\hat{S}_3 - 2J_{23}\hat{S}_2\hat{S}_3 \quad (7)$$

(31) Kambe, K. *J. Phys. Soc. Jpn.* 1950, 5, 48.
(32) Griffith, J. S. *Struct. Bonding (Berlin)* 1972, 10, 87 and references therein.

A Hexanuclear Ferric Complex with a S = 5 Ground State

J. Am. Chem. Soc., Vol. 113, No. 16, 1991 6121

The reason for this is that there is no way to couple the spins in such a system to *uniquely* describe the spin state of the molecule.

This same situation is found when one tries to generate a set of vectors to yield an operator-equivalent expression for eq 2. Since each pairwise interaction in complex **3** is in the strictest sense gauged by its own coupling constant, the analogy between complex **3** as described by eq 1 and a 3-*J* triangle is clear. However, even if one were to make some simplifying assumptions and allow certain of the pairwise interactions in complex **3** to be described by the same *J* terms, the problem remains unchanged. For example, a somewhat reasonable approximation to make would be to set $J_{31'} = J_{21'}$. The resulting spin Hamiltonian is given in eq 8.

$$\hat{H} = -2J_{12}(\hat{S}_1 \cdot \hat{S}_2 + \hat{S}_{1'} \cdot \hat{S}_{2'}) -$$
$$2J_{23}(\hat{S}_2 \cdot \hat{S}_3 + \hat{S}_{2'} \cdot \hat{S}_{3'} + \hat{S}_3 \cdot \hat{S}_{1'} + \hat{S}_{3'} \cdot \hat{S}_1) - 2J_{21'}(\hat{S}_2 \cdot \hat{S}_{1'} + \hat{S}_{2'} \cdot \hat{S}_1)$$
$$(8)$$

Even with this simplification, the only way to make an operator replacement in eq 8 is with a set of nonlinearly independent equations. The origin of the problem in complex **3** lies in the fact that the four Fe^{III} ions making up the central plane of the molecule are involved in two distinctly different types of spin–spin interactions. Thus, it will always be the case that the spin operators for these four ions will appear in at least two vector definition equations: one for the μ_2-OH pathway and one for the μ_3-O pathway. As such, the Kambe approach fails for this molecular topology, and a linearly independent description of the spin-state manifold is not obtainable by this route.

In terms of describing the entire magnetic structure of complex **3** and extracting values for the various coupling constants, the failure of the Kambe approach leaves essentially two options. The first employs a molecular-field approximation, whereby we would assume that the strongest spin–spin coupling exists within the Fe^{III} triangles and that the μ_2-OH pathways represent extremely weak interactions. We feel that the molecular-field approximation would *not* be appropriate in the present case. Although it is likely that the μ_2-OH pathway is the weakest of all the interactions present in complex **3**, we do not feel this interaction is so weak compared to the μ_3-O pathway that we can employ this simplification. This conclusion is based largely upon an examination of the Fe^{III}–bridge–Fe^{III} distances, which Gorun and Lippard[33] and more recently Que and co-workers[34] have empirically established to be of primary importance in determining the strength of spin–spin interactions in high-spin Fe^{III} clusters. While the average Fe^{III}–μ_2-OH distance is somewhat longer than the average Fe–μ_3-O distance (ca. 1.96 Å versus 1.91 Å, respectively), we do not feel that the difference is such that the molecular-field approximation is justified.

The second and by far most rigorous approach is diagonalization of the complete spin Hamiltonian for the system. The 46 656 × 46 656 matrix required to describe complex **3** makes the task intractable in practical terms. In fact, the largest spin system to be handled by this approach to date is a tetranuclear high-spin Mn^{II} complex.[35] The spin degeneracy of that system is 1296, vastly smaller than the problem under consideration here.

Variable-Field Magnetization Studies. Even though a quantitative description of the entire spin manifold of complex **3** is not yet possible, the nature of the ground state can be determined by looking at the magnetization of the compound at low temperature as a function of applied magnetic field. A plot of the reduced magnetization $M/N\mu_B$ versus H/T for complex **3**·CH_2Cl_2, where N is Avogadro's number and μ_B is the Bohr magneton, is given in Figure 5. The data indicate that at high field and low temperature (1.57 K at 40.00 kG) the reduced magnetization plateaus at a value of ca. 9.2. This value is close to the saturation value of 10 expected for an isolated $S = 5$ state. The fact that the three
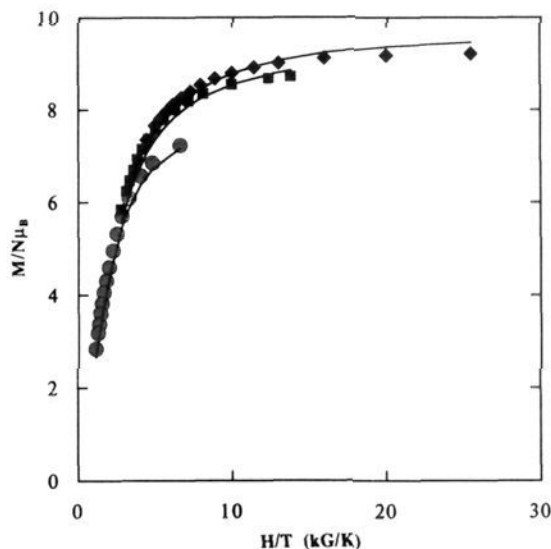
Figure 5. Plots of reduced magnetization versus magnetic field in units of temperature for $[Fe_6O_2(OH)_2(OAc)_{10}(C_{10}H_{13}N_4O)_2]\cdot CH_2Cl_2$ (**3**·CH_2Cl_2, sample c): circles, 10.00 kG; squares, 25.00 kG; tilted squares, 40.00 kG. The solid lines indicate fits to a zero-field split $S = 5$ state. See text for details.

isofield lines do not superimpose indicates that the ground state is split in zero-field.

The solid lines in Figure 5 represent the best fit of the data to a spin Hamiltonian for an isolated $S = 5$ state under the influence of axial zero-field splitting of the form $\hat{H}_{zfs} = D\hat{S}_z^2$. The data at all three fields were simultaneously fit by a full-matrix diagonalization of the Hamiltonian for both parallel ($H_\parallel$) and perpendicular ($H_\perp$) conponents of the applied field; the g value was assumed to be isotropic. The parameters giving the best fit of all three isofield data sets are $g = 1.94$ and $D = 0.22$ cm^{-1} with a fixed temperature-independent paramagnetic contribution of 8.00×10^{-4} cgsu. A weighting scheme was used to provide for an equal distribution of data points in H/T (i.e., no one region of H/T was emphasized more than any other on the basis of density of data points). The positive value of D indicates a stabilization of the $m_s = 0$ component of the $S = 5$ state, consistent with the low-temperature drop in μ_{eff} observed in the bulk susceptibility data (see Figure 3). It can be seen that the fit is quite good overall, although it is possible that due to the low symmetry of the molecule there is a small rhombic component ($E[\hat{S}_x^2 - \hat{S}_y^2]$) to the zero-field perturbation. However, the present quality of the fit does not warrant the inclusion of another parameter. The small value for D is consistent with expectations for a system composed of high-spin Fe^{III} ions. Similar analyses of the magnetization data were attempted for spin Hamiltonians appropriate for $S = 4$ and $S = 6$ ground states. Although the quality of these fits is comparable to that found for the $S = 5$ analysis, *the g values calculated were unreasonable for a system of high-spin* Fe^{III} ions. Fitting for $S = 4$ gave $g = 2.39$ ($D = 0.31$ cm^{-1}), and for $S = 6$ a best fit was found for $g = 1.63$ ($D = 0.16$ cm^{-1}); the TIP values as well as the weighting schemes were identical in each case with those used for the $S = 5$ fit. Thus, it is clear that complex **3** does have a $S = 5$ ground state that is reasonably well isolated, as was implied from the variable-temperature 10.00-kG susceptibility data.

In Figures 6 and 7 are shown plots from the matrix diagonalization of the eigenvalues as a function of field strength in $H_\parallel$ and $H_\perp$, respectively. The experimentally observed saturation of the magnetization at 40.00 kG is substantiated from these plots, since the $m_s = -5$ component of the $S = 5$ state becomes the only state populated at low temperature for $H_\parallel$ due to the large Zeeman interaction (see Figure 6). The reduction in the reduced magnetization relative to the expected saturation value of 10 is due to the off-diagonal mixing of m_s states with $H_\perp$. While nominally of $m_s = 0$ parentage, the lowest energy state with $H_\perp$

(33) Gorun, S. M.; Lippard, S. J. *Recl. Trav. Chim. Pays-Bas* **1987**, *106*, 417.

(34) Norman, R. E.; Holz, R. C.; Ménage, S.; O'Connor, C. J.; Zhang, J. H.; Que, L., Jr. *Inorg. Chem.* **1990**, *29*, 4629.

(35) Aussoleil, J.; Cassoux, P.; de Loth, P.; Tuchagues, J.-P. *Inorg. Chem.* **1989**, *28*, 3051.
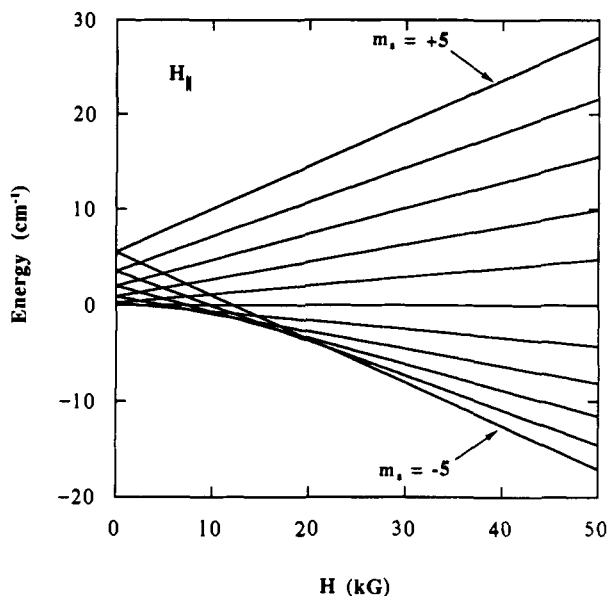
Figure 6. Plots of the eigenvalues with $H_\parallel$ derived from a fit of the magnetization data for $[Fe_6O_2(OH)_2(OAc)_{10}(C_{10}H_{13}N_4O)_2]\cdot CH_2Cl_2$.
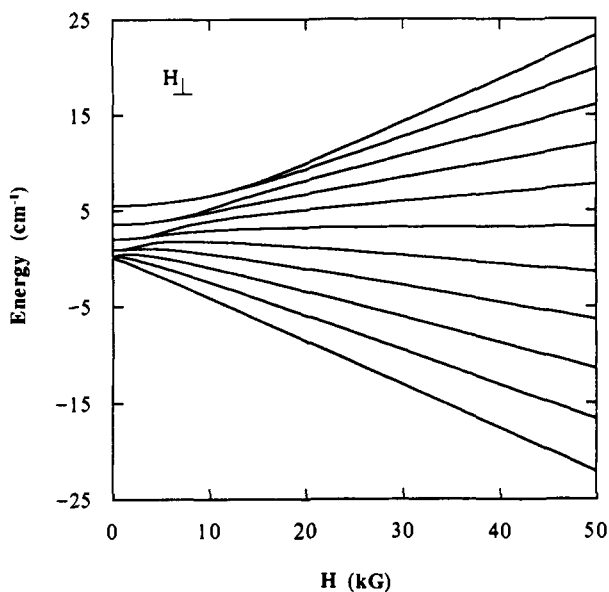
Figure 7. Plots of the eigenvalues with $H_\perp$ derived from a fit of the magnetization data for $[Fe_6O_2(OH)_2(OAc)_{10}(C_{10}H_{13}N_4O)_2]\cdot CH_2Cl_2$.

shows a marked field dependence due to extensive field-induced mixing with non-zero m_s components of the ground state (see Figure 7). At 40.00 kG, the wave function Ψ of this state is given by eq 9, where we have used the bracket notation to identify the

$$\psi = -0.1842\ |\text{-}5> - 0.2511\ |\text{-}4> + 0.4451\ |\text{-}3> + 0.5056\ |\text{-}2> +$$

$$0.0559\ |\text{-}1> + 0.4492\ |0> - 0.4143\ |1> - 0.2093\ |2> -$$

$$0.1631\ |3> + 0.0444\ |4> + 0.0168\ |5>   \qquad (9)$$

various parent m_s states. Thus, the field-induced mixing of m_s states in this compound is quite complicated and is a direct consequence of the high-spin nature of the ground state of this molecule.

Nature of the $S = 5$ Ground State: Spin Frustration. In the case of the hexanuclear complex 5, it was concluded[6f,g] on the basis of bulk susceptibility data that the ground state is diamagnetic; i.e., $S = 0$. Although no theoretical treatment was put forth, it was very reasonable for Micklitz et al.[6f,g] to rationalize the origin of this ground state in terms of the well-documented antiferromagnetic nature of pairwise Fe^{III}–Fe^{III} interactions when mediated by oxide, hydroxide, or alkoxide bridges. However, if one examines

the topology of both complex 3 and complex 5, it is by no means obvious that a $S = 0$ state should be the ground state of complex 5. As we have pointed out previously,[22,36] the notion of spin frustration can play a vital role in determining the magnetic structure of polynuclear transition-metal complexes. Frustration in triangulated systems is quite easily understood, but the same type of frustration can occur in complexes with an even number of metal centers.[22,36] As an example, consider the topology of complex 5, which is, of course, similar to that of complex 3. If one ascribes an antiferromagnetic coupling to each of the pairwise interactions starting with any Fe^{III} site and continues around the periphery of the complex, there is no difficulty in arriving at a spin configuration having $S = 0$. However, upon examining the
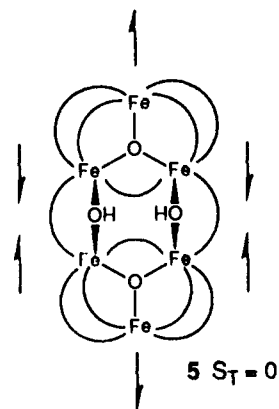
resulting spin distribution, it becomes clear that two of the interactions, specifically those of the ions involved in both the μ_3-O and μ_2-OH bridges, are *spin-aligned* with respect to the μ_3-O pathway. This result, and the subsequent ambiguity in spin polarization, is the essence of spin frustration and is an inescapable consequence of this nuclear arrangement.

As was indicated above, there are 581 different $S = 5$ states in the spin manifold of complex 3. In the absence of any information regarding the magnitude of the various pairwise interactions, it is not possible to identify the spin distribution responsible for this novel configuration. However, since $S = 5$ represents neither the minimum ($S = 0$) nor the maximum ($S = 15$) spin state available in this complex, we describe this ground state as possessing an intermediate spin value. Such intermediate values can come about when competition between multiple coupling pathways results in a partial or complete frustration of the intrinsic character of a given interaction. To illustrate this concept and understand how it applies in the present case, we consider once again a triangular arrangement of Fe^{III} ions bridged by a central μ_3-O:
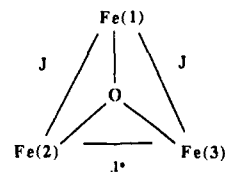
For the sake of the following discussion, we will assume that we are dealing with a spin system described by eqs 5 and 6, which we rewrite as

$$\hat{H} = -2J(\hat{S}_1\cdot\hat{S}_2 + \hat{S}_1\cdot\hat{S}_3) - 2J^*(\hat{S}_2\cdot\hat{S}_3)   \qquad (10)$$

$$\hat{H} = -J(\hat{S}_T^2 - \hat{S}_A^2 - \hat{S}_1^2) - J^*(\hat{S}_A^2 - \hat{S}_2^2 - \hat{S}_3^2)   \qquad (11)$$

or more simply

$$\hat{H} = -J(\hat{S}_T^2 - \hat{S}_A^2) - J^*(\hat{S}_A^2)   \qquad (12)$$

where we have dropped the constant single-ion $\hat{S}_i^2$ terms. In Figure

(36) McCusker, J. K.; Vincent, J. B.; Schmitt, E. A.; Mino, M. L.; Shin, K.; Coggin, D. K.; Hagen, P. M.; Huffman, J. C.; Christou, G.; Hendrickson, D. N. *J. Am. Chem. Soc.* **1991**, *113*, 3012.

A Hexanuclear Ferric Complex with a S = 5 Ground State

J. Am. Chem. Soc., Vol. 113, No. 16, 1991 6123
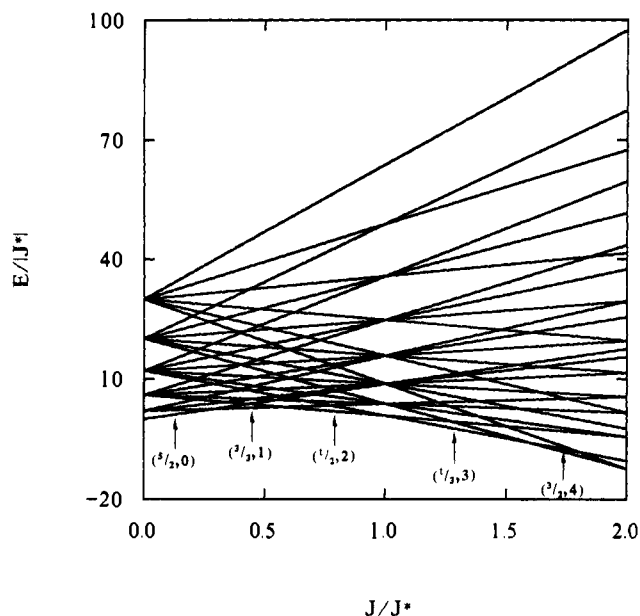
Figure 8. Plots of the eigenvalues of eq 12 for a triangular array of Fe^{III} ions in units of J^*. The states are labeled as (S_T, S_A). See text for details.

8 are plotted the energies of all 27 eigenstates of eq 12 ranging in S_T from $^1/_2$ to $^{15}/_2$ in units of $|J^*|$ as a function of the ratio J/J^*. The diagram was constructed for J and $J^* < 0$, i.e., both exchange interactions being antiferromagnetic. There are several items concerning Figure 8 that should be noted. The most obvious fact is that the overall magnetic structure of this type of system is reasonably complicated and, more importantly, is *extremely* sensitive to the ratio J/J^*. It can be seen that there are a total of six different ground states possible (the ground state being defined by the bottom line for a given point along the x axis), spanning three different values of S_T. These S_T values are $^1/_2$, $^3/_2$, and $^5/_2$.

The most useful way to interpret this diagram is to consider movement along the x axis as a means of varying the degree of spin frustration present in the system with respect to the two coupling pathways. If the J^* coupling is much stronger than J ($J/J^* \leq 0.3$), the ground state is described by $S_T = ^5/_2$ and $S_A = 0$. The value of S_A indicates that the spin vectors $\hat{S}_2$ and $\hat{S}_3$ are completely paired up. The result is complete frustration of the J-coupling pathway. Even though this interaction is intrinsically antiferromagnetic, the relative strength of the J^* interaction causes a net spin polarization whereby the ions involved in the J pathways are actually *spin-aligned*. As the strength of the J coupling pathway increases relative to J^* (i.e., for $0.3 \leq J/J^* \leq 0.55$), a $S_T = ^3/_2$ ground state results. The value of $S_A = 1$, which contributes to this state, is one of the vector-coupled combinations spanned by the $(\hat{S}_2 + \hat{S}_3)$ sum which defines $\hat{S}_A$. Since this sum can range from 0 to 5, a value of 1 indicates a strong tendency for the spin vectors to align antiparallel. However, the spins on Fe(2) and Fe(3) cannot completely pair up to 0, as in the case of the $S_T = ^5/_2$ state, because of the now appreciable J-type interaction. As we further increase the relative strength of J, a $S_T = ^1/_2$ state develops for which $S_A = 2$. Again, the tendency is for $\hat{S}_2$ and $\hat{S}_3$ to pair up, but it becomes increasingly more difficult due to the presence of the J interaction and the competing tendency to antiferromagnetically align the Fe(1)/Fe(2) and Fe(1)/Fe(3) pairs.

A turning point is reached for $J/J^* = 1.0$. At this stage, the two interactions are of equal magnitudes and eq 12 collapses to $\hat{H} = -J\hat{S}_T^2$, appropriate for an equilateral arrangement of the ions. Now, as J/J^* increases, it is the J^* interaction that becomes frustrated as the tendency to spin-pair the J-type interactions overrides the antiferromagnetic nature of J^*, producing ground states with consistently larger values for $\hat{S}_A$. Thus, for values of J/J^* between 1.0 and 1.6, the ground state is given by $S_T = ^1/_2$

and $S_A = 3$; $S_T = ^3/_2$ and $S_A = 4$ are found for $1.6 \leq J/J^* \leq 2.0$, and $S_T = ^5/_2$ and $S_A = 5$ for $J/J^* > 2.0$. The last configuration represents the opposite extreme to the other $^5/_2$ state, in that the J interaction is dominant to the point of negating the J^* interaction, yielding a completely spin-parallel configuration for Fe(2) and Fe(3) spin vectors.

With these results in mind, let us now consider the situations present in the hexanuclear complexes being examined here. In view of the fairly high symmetry of complex 5, the region about $J/J^* = 1$ would seem to be of particular importance with regard to the magnetism observed for this complex. It is by no means obvious that in the triangulated system for $J = J^*$ one should have a ground state with $S_T = ^1/_2$; spin frustration is clearly present in states with $S_A = 2$ or 3, and this naturally leads to difficulties in conceptualizing the origin of the ground state. However, it is clear from the above analysis of the trinuclear case that the lowest spin state of the system is the most stable under these conditions. What we may conclude on the basis of our empirical observations and these calculations is the following: as all of the coupling pathways become more equivalent in these types of systems, the intrinsically antiferromagnetic nature of the spin–spin interactions serve to drive the system to a state of minimum unpaired spin density. We believe that the origin of the $S = 0$ ground state in complex 5 is a manifestation in large part of the symmetry of that molecule. In particular, the intratriangle coupling pathways, being very nearly equivalent on the basis of bond distances, are likely all very similar. The system thus tends to fall into a state of minimum spin density, which in this case is characterized by $S = 0$. With 111 $S = 0$ states available, it is not easy to specify the exact makeup of this state in lieu of any knowledge about the values of each of the coupling constants. The ground state likely arises from intermediate vector-coupled components, as in the $S_T = ^1/_2$ states of the Fe^{III}_3 complexes, and as such would be difficult to represent. However, we suggest that the same tendency which produces a $S = ^1/_2$ ground state in a symmetric Fe_3O system is operative in complex 5 as well.

This notion of the symmetry of the various exchange interactions is likely the origin of the $S = 5$ state observed for complex 3, as well. The presence of the μ_2-alkoxide pathway breaks the symmetry of the exchange interactions within the two iron triangles. The net result is the possibility that one interaction may become stronger than another, thereby skewing the coupling ratios and causing the system to move away from a minimum spin density state to one that favors the dominant pathway. The dominant exchange pathway is probably not the μ_2-alkoxide alone due to the long Fe–μ_2-O distances present. However, the alkoxide bridge does cause asymmetric structural changes within the iron triangle (vide supra) as well as presenting an additional, albeit weak, secondary exchange pathway. As is evident from Figure 8, only minor changes in the ratios of coupling constants are required to cause substantial changes in the magnetic structure of a complex. The only other major difference in the topology of complex 3 as compared to complex 5 is the orientation of the μ_2-OH groups relative to the central iron plane. Although this difference is intriguing from a structural point of view, it is not clear to us how a syn versus anti arrangement of these bridges will affect an exchange interaction that is presumed to occur via a superexchange mechanism. Whatever the specific origin, we feel that the hydroxy diimidazole ligand 1 presents a sufficient perturbation to the hexanuclear Fe^{III} spin system relative to the previously reported complex 5 to bring about a novel magnetic ground state.

Concluding Comments

The synthesis and X-ray structure of hexanuclear Fe^{III} complex 3 are reported. It was shown that this complex consists of two μ_3-oxo Fe^{III}_3 triangular complexes bridged together at two vertices. Fitting of variable-field magnetization data shows that complex 3 has a $S = 5$ ground state. This is very unusual for a complex of high-spin ferric ions, for pairwise magnetic exchange interactions between high-spin Fe^{III} ions are invariably antiferromagnetic. Spin frustration is shown to be the likely origin of the $S = 5$ ground state for complex 3. Thus, each of the two Fe^{III}_3 triangular units

that make up complex **3** is a scalene triangle and spin frustration results.

It should be possible to prepare additional polynuclear iron and manganese complexes that have ground states with large numbers of unpaired electrons. This can be done by designing the polynuclear complex so that it exhibits spin frustration. The complex $[Mn^{IV}_4Mn^{III}_8O_{12}(O_2CPh)_6(H_2O)_4]$ probably also has a $S = 14$ ground state due to spin frustration.[8f,22,36]

Note Added in Proof. For a recent report of the preparation of diimidazole **1**, see: Byers, P. K.; Canty, A. J. *Organometallics* **1990**, *9*, 210.

Supplementary Material Available: Tables of complete bond lengths and bond angles, anisotropic thermal parameters, calculated hydrogen atom positions, and magnetic susceptibility data and a stereoview of complex **3**·8CH$_2$Cl$_2$ (10 pages); a listing of observed and calculated structure factors for complex **3**·8CH$_2$Cl$_2$ (20 pages). Ordering information is given on any current masthead page.

Nitridoosmium(VI) and Nitridoruthenium(VI) Complexes of Cysteine(2-) and Related Ligands

Joseph J. Schwab, Elizabeth C. Wilkinson, Scott R. Wilson, and Patricia A. Shapley*

Contribution from the School of Chemical Sciences, University of Illinois, Urbana, Illinois 61801. Received February 4, 1991

Abstract: Anionic complexes of nitridoruthenium(VI) and nitridoosmium(VI) containing covalently bound *N*-acetyl-L-cysteinato, 3-sulfidopropionato, and 3-sulfidopropionamidato ligands have been synthesized to model the binding of δ-(L-α-aminoadipyl)-L-cysteinyl-D-valine to the iron center in the metalloenzyme isopenicillin N synthetase. The complexes are prepared by the reaction of *N*-acetyl-L-cysteine, 3-mercaptopropionic acid, and 3-mercaptopropionamide with [NBu$^n_4$][Os(N)(OSiMe$_3$)$_4$], [NBu$^n_4$][Os(N)Cl$_4$], [NBu$^n_4$][Ru(N)(CH$_2$SiMe$_3$)$_4$], or [NBu$^n_4$][Ru(N)(OSiMe$_3$)$_4$]. They have been characterized by elemental analysis and IR and NMR spectroscopy. Spectroscopic data show that the *N*-acetyl-L-cysteinato and 3-sulfidopropionato ligands are bound to the metal center through sulfur and oxygen, while the 3-sulfidopropionamidato ligands are bound through sulfur and nitrogen. The molecular structures of *cis*-[NBu$^n_4$][Os(N)(O$_2$CCH$_2$CH$_2$S)$_2$], [NBu$^n_4$][Os(N){O$_2$CCH(NHCOCH$_3$)CH$_2$S}$_2$], and [PPh$_4$][Ru(N)(NHCOCH$_2$CH$_2$S)$_2$)] were determined by single-crystal X-ray diffraction. These complexes were found to have distorted square-pyramidal geometry around the metal center. *cis*-[NBu$^n_4$][Os(N)(O$_2$CCH$_2$CH$_2$S)$_2$] crystallizes in monoclinic space group $P2_1/c$ with $a = 13.718$ (6) Å, $b = 10.080$ (3) Å, $c = 19.890$ (5) Å, $\beta = 92.16$ (3) Å, and $Z = 4$. [NBu$^n_4$][Os(N){L-O$_2$CCH(NHCOCH$_3$)CH$_2$S}$_2$] crystallizes in monoclinic space group $C2$ with $a = 18.371$ (6) Å, $b = 9.261$ (1) Å, $c = 21.125$ (7) Å, $\beta = 102.92$ (3) Å, and $Z = 4$. [PPh$_4$][Ru(N)(NHCOCH$_2$CH$_2$S)$_2$)] crystallizes in orthorhombic space group *Pbca* with $a = 23.022$ (1) Å, $b = 16.120$ (1) Å, $c = 15.728$ (1) Å, and $Z = 8$.

Introduction

The biological importance of metal–cysteine interactions has led to a great deal of activity in the study of the coordination chemistry of cysteine and related molecules. Coordination of cysteine to a metal center has been shown to occur in a number of metalloenzymes. These include enzymes involved in the synthesis of β-lactam antibiotics, such as isopenicillin N synthetase,[1] and those causing the decomposition of these antibiotics, such as β-lactamase II.[2] Present evidence suggests that the first step in the oxidative cyclization of δ-(L-α-aminoadipoyl)-L-cysteinyl-D-valine to isopenicillin N is the coordination of the substrate to the iron atom, through the cysteinyl sulfur and the valinyl amide nitrogen. Coordination of the cysteine thiolate to an iron center is known to occur in cytochrome P-450,[3] ω-hydroxyase,[4] chloro-

peroxidase,[5] subunit II of bovine cytochrome *c* oxidase,[6] and iron–sulfur electron transport proteins.[7]

Main group metal and transition metal complexes of cysteine and cysteine derivatives have been prepared and isolated.[8] In general, these are insoluble or sparingly soluble materials and have been characterized mainly by elemental analysis and IR spectroscopy. On the basis of their infrared spectra, these complexes were proposed to have monodentate (S), bidentate (N,S), bidentate (O,S), tridentate (O,N,S), or bridging bonding modes.[9] The

(1) (a) Baldwin, J. E.; Bradley, M. *Chem. Rev.* **1990**, *90*, 1079–1088. (b) Chen, V. J.; Orville, A. M.; Harpel, M. R.; Frolik, C. A.; Surerus, K. K.; Munck, E.; Lipscomb, J. D. *J. Biol. Chem.* **1989**, *264*, 21677–21681. (c) Ming, L.; Que, L., Jr.; Kriauciunas, A.; Frolik, C. A.; Chen, V. J. *Inorg. Chem.* **1990**, *29*, 1111–1112.

(2) Sovago, I.; Martin, R. B. *J. Inorg. Nucl. Chem.* **1981**, *43*, 425–429.

(3) (a) Hanson, L. K.; Eaton, W. A.; Sligar, S. G.; Gunsalus, I. C.; Gouterman, M.; Connel, C. R. *J. Am. Chem. Soc.* **1976**, *98*, 2672–2674. (b) Cramer, S. P.; Dawson, J. H.; Hodgson, K. O.; Hager, L. P. *J. Am. Chem. Soc.* **1978**, *100*, 7282–7290. (c) White, R. E.; Coon, M. J. *Annu. Rev. Biochem.* **1980**, *49*, 315–356. (d) Hahn, J. E.; Hodgson, K. O.; Andersson, L. A.; Dawson, J. H. *J. Biol. Chem.* **1982**, *257*, 10934–10941. (e) Champion, P. M.; Stallard, B. R.; Wagner, G. C.; Gunsalus, I. C. *J. Am. Chem. Soc.* **1984**, *106*, 5469–5472. (f) Tsubaki, M.; Tomita, S.; Tsuneoka, Y.; Ichikawa, Y. *Biochim. Biophys. Acta* **1986**, *870* (3), 564–574. (g) Poulos, T. J. In *Cytochrome P-450: Structure, Mechanism and Biochemistry*; Ortiz de Montellano, P. R., Ed.; Plenum Press: New York, 1986; Chapter 13. (h) Poulos, T. In *Hemeproteins, 7*; Eichhorn, G. L., Marzilli, L. G., Eds.; Elsevier Press: New York, 1988; p 13.

(4) Ruettinger, R. T.; Griffith, G. R.; Coon, M. J. *Arch. Biochem. Biophys.* **1977**, *183*, 528–537.

(5) (a) Dawson, J. H.; Trudell, J. R.; Barth, G.; Linder, R. E.; Bunnenburg, E.; Djerassi, C.; Chiang, R.; Hager, L. P. *J. Am. Chem. Soc.* **1976**, *98*, 3709–3710. (b) Cramer, S. P.; Dawson, J. H.; Hodgson, K. O.; Hager, L. P. *J. Am. Chem. Soc.* **1978**, *100*, 7282–7290. (c) Champion, P. M.; Gunsalus, I. C.; Wagner, G. C. *J. Am. Chem. Soc.* **1978**, *100*, 3743.

(6) Darley-Usmar, V. M.; Capaldi, R. A.; Wilson, M. T. *Biochim. Biophys. Res. Commun.* **1982**, *108* (4), 1649–1654.

(7) Thomas, A. J. Iron Sulfur Proteins. In *Metalloproteins Part I: Metal Proteins with Redox Roles*; Harrison, P., Ed.; MacMillan: London, 1985; pp 79–120.

(8) (a) Li, N. C.; Manning, R. A. *J. Am. Chem. Soc.* **1955**, *77*, 5225–5228. (b) White, J. M.; Manning, R. A.; Li, N. C. *J. Am. Chem. Soc.* **1956**, *78*, 2367–2370. (c) Sharma, C. L.; De, T. K. *J. Indian Chem. Soc.* **1982**, *59*, 101–103. (d) Masoud, M. S.; Abdel-Nabby, B. A.; Soliman, E. M.; Abdel-Hamid, O. H. *Thermochim. Acta* **1988**, *128*, 75–80. (e) Makni, C.; Aplincourt, M.; Hugel, R. P. *J. Chem. Res., Synop.* **1980**, 354–355. (f) Claude, M.; Paris, M.; Scharff, J. P.; Aplincourt, M.; Hugel, R. P. *J. Chem. Res., Synop.* **1981**, 222–223. (g) Kozlowski, H.; Decock-Le Reverend, B.; Ficheux, D.; Loucheux, C.; Sovago, I. *J. Inorg. Biochem.* **1987**, *29*, 187–97.